

AD620680

Division of Engineering Mechanics

STANFORD UNIVERSITY

Technical Report No. 155

FOR INFORMATION			
DATE			
PRICE			
\$3.00	0.75	96	ed
ARCHIVE COPY			

BUCKLING OF SHALLOW VISCOELASTIC ARCHES

by

D. L. Anderson

DDC
SEP 17 1965
TISA B

August 1965

Prepared under Office of Naval Research

Contract Nonr 225(69)

Project Report No. 8

Division of Engineering Mechanics
STANFORD UNIVERSITY

Technical Report No. 155

BUCKLING OF SHALLOW VISCOELASTIC ARCHES

by

D. L. Anderson

August 1965

Prepared under Office of Naval Research

Contract Nonr 225(69)

Project Report No. 8

ABSTRACT*

A method of solution to the buckling problem for shallow viscoelastic shells is presented. The arches are considered to be pin-ended at rigid supports, of arbitrary initial shape but of uniform cross section, and made of an arbitrary linear viscoelastic material. The lateral loading may be an arbitrary function of both position and time.

Specific solutions are given for several arches to point out the influence of the material and of asymmetries in the initial arch shape on the deformation and buckling time of the system. Two types of viscoelastic material, the Maxwell Fluid and the three parameter solid, are included in the examples.

The viscoelastic property of the material in the analysis is expressed in integral operator form, which is shown to lead to simple numerical time integrations in determining the arch deflection, as well as maintaining the form of the governing equations that determine stability in the same general form as the equations of an elastic arch. The method of solution takes into account the fact that the arch may buckle in either a symmetrical or an unsymmetrical mode.

It is seen that arches composed of a viscoelastic solid

*The results communicated in this paper were obtained in the course of an investigation conducted under Contract Nonr 225(69) by Stanford University with the Office of Naval Research, Washington, D. C. Reproduction in whole or in part is permitted for any purposes of the United States Government.

material may, if the load is not too great and constant for time large, reach a final unbuckled position as the time becomes very large. If this is the case then it is shown that the time integration that previously required numerical integration can now be approximated analytically. Several examples are given.

TABLE OF CONTENTS

	page
CHAPTER I: Introduction and Summary	1
CHAPTER II: Linear Viscoelastic Materials	21
CHAPTER III: General Analysis	26
CHAPTER IV: Sinusoidal Arch under Sinusoidal Loading	39
CHAPTER V: Non-sinusoidal Arch	53
(V.I) Two modes excited	53
(V.II) Several modes excited	66
CHAPTER VI: Long-time Solution for a Viscoelastic Solid Material	75
CHAPTER VII: General Features of the Numerical Solution	83
REFERENCES	86

NOTATION

A	cross-sectional area of the arch
A_m	$= a_m \frac{L}{2} \sqrt{\frac{A}{I}}$, dimensionless coefficients in the Fourier expansion of the initial arch shape
$B_m(\tau)$	$= b_m(\tau) \frac{L}{2} \sqrt{\frac{A}{I}}$, dimensionless functions of time in the Fourier expansion of the arch position
C	constant
E	elastic modulus
$E(t)$	relaxation function of the viscoelastic material
E_0	$= E(0)$, initial modulus
E_F	$= E(\infty)$, final modulus
$E^*(\tau_n, \tau_{n-1})$	$= \frac{E(\tau_n - \tau_{n-1}) - E_0}{2E_0}$
$H(t)$	$= \left\{ \begin{array}{ll} 0 & \text{for } t < 0 \\ 1 & \text{for } t \geq 0 \end{array} \right\}$, unit step function
I	arch moment of inertia
L	span of arch or column length
$M(x, t)$	moment on arch
P	concentrated load on column or arch
P_{cr}, P_{cr}^F	critical values of P that cause buckling
$P(t)$	arch thrust
$R_m(t)$	dimensionless load parameters in the Fourier expansion of the lateral load
$R_u(\tau), R_s(\tau)$	critical values of $R_1(\tau)$ that cause buckling
ΔR_m	psuedo load used to check stability
$S(\tau), S_m(\tau)$	dimensionless time functions that depend on the previous history of the arch deflection

a_m	dimensionless coefficients in the Fourier expansion of the initial arch shape
$b_m(t)$	dimensionless time functions in the Fourier expansion of the arch position
$f(P,t)$	dimensionless time function depending on the viscoelastic material and the column load
$q(x,t)$	lateral load
q_0	$= \frac{2\pi^4 E_0 I}{L^4} \sqrt{\frac{I}{A}}$, a constant with the same units as $q(x,t)$
t	time
x,y	cartesian coordinates
$y(x,t)$	position of arch centroidal axis
$y_0(x)$	$= y(x,0^-)$, initial position of arch
$\delta, \delta(t)$	midpoint deflection of arch or column
δ_0	initial position of midpoint of arch or column
$\epsilon, \epsilon_0, \epsilon(t)$	strain
ζ	distance of a material point from the centroidal axis of the arch
η	viscosity of dashpot in material models, units of FT/L^2
$\sigma, \sigma(t)$	stress
τ	$= t/\text{relaxation time of the material}$, dimensionless time

Chapter I Introduction and Summary

Whenever a structure or structural member is subject to compressive loads, the possibility of an instability type of failure must be considered. Many structures, when loaded to a critical state, will undergo a marked change in the magnitude and character of their deformation, which is not the result of any failure or alteration in the mechanical properties of the material. Such a change generally occurs because one mode of deformation becomes unstable and the structure deflects to another, stable mode. This change is termed buckling, and the loading associated with this critical state is most generally called the buckling load. However, there are many structures for which a well defined buckling load does not exist. For these structures the useful load carrying ability must be based on other factors, such as maximum allowable stresses or deflections.

Structures that are made of materials which do not exhibit any time effects have a buckling load that is independent of time provided the load is applied slowly enough so that the response can be considered as static. However, viscoelastic structures, because the material exhibits time or memory effects in that the strain is a function of the stress history, may have a buckling load that is a function of time even for a quasi-static analysis of the problem. Moreover, for structures that exhibit no well defined buckling action, viscoelastic material properties can greatly

influence their load carrying ability, especially if the deformations tend to reduce the stiffness of the structure.

Buckling occurs most often in structures that have at least one dimension small in comparison to the other two; for massive structures not falling into this class, material failure more commonly provides the critical condition on the magnitude of loading. An explanation of why this is so can be seen by investigating the relationship between elastic stability theory and linear elasticity theory. In elasticity theory, the equations of equilibrium are written for the body in its undeformed state. If the body is massive it cannot undergo large deformations without large strains, and since elastic strains for most engineering materials are very small it is concluded that the deformations must be very small and can be neglected in writing the equations of equilibrium. This approach then leads to the linear equations of elasticity which have a unique solution, and as such cannot describe a stability problem. By contrast, in stability theory the equations of equilibrium must be written for the body in its deformed state. Slender bodies can undergo large deformations without producing large strains, and consequently the deformations must be accounted for when writing the equilibrium equations, since they are no longer restricted to being small.

It is possible to distinguish several different kinds of buckling, depending on the type of structure and the manner of loading. By far the most widely studied type is the

so-called classical buckling, an example of which is the centrally loaded straight column. A second type is snap-through buckling, which occurs in structures whose resistance to an increase in load decreases as the loading or the deformations increase. An example of this is the laterally loaded shallow arch, the analysis of which, for the viscoelastic case, forms the body of this dissertation.

The classical buckling problem of the centrally loaded straight column, as well as the problem of the initially imperfect column which has no well defined buckling load, has been studied in detail for both elastic and viscoelastic materials (see references [1]¹ through [9]). Because there are essential differences in the responses between an elastic and a viscoelastic column, the results of some of the above references will be outlined here.

Consider a centrally loaded straight elastic column as shown in Fig. 1.1a. As the load P increases the column remains perfectly straight until $P = P_{cr}$. If $P = P_{cr}$, the column may deflect laterally as shown in Fig. 1.1b, and any value of δ is an equilibrium position. P_{cr} is then the critical load at which a change in deformation may occur.

¹Numbers in square brackets [] refer to the list of References.

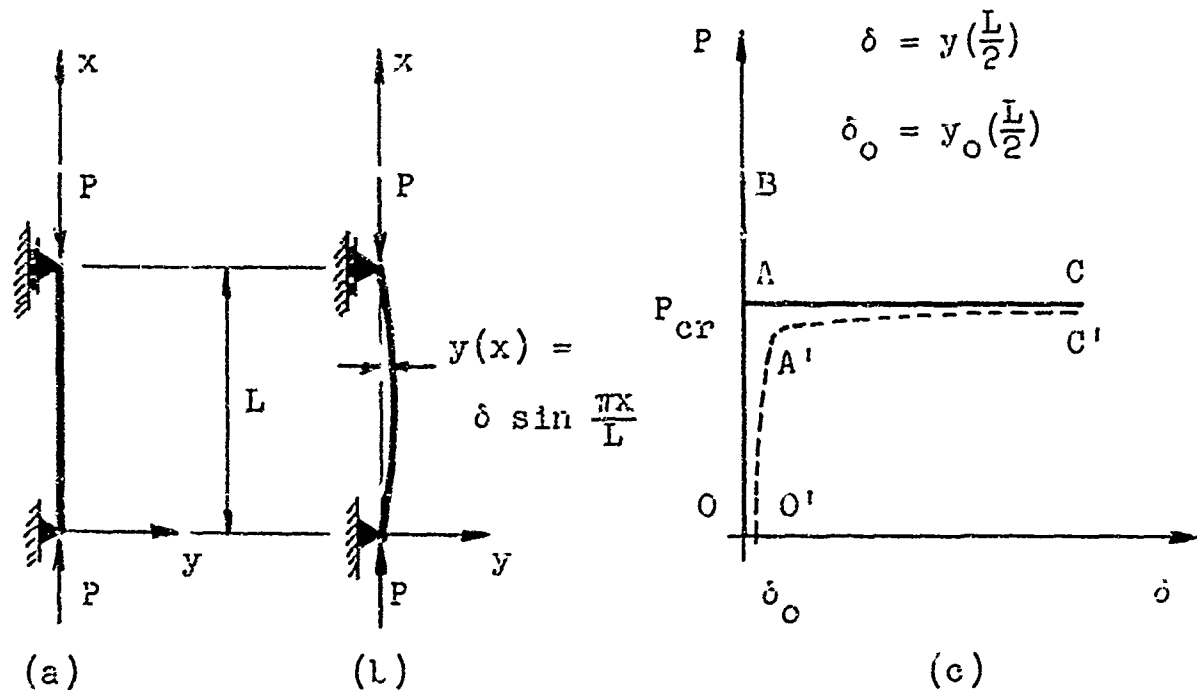


Fig. 1.1

The solid curves, OAB and OAC of Fig. 1.1c show the load vs. lateral deflection parameter δ , where δ is the value of the deflection at the midheight of the column. At the point A there exist two different equilibrium paths of deformation. This condition is referred to as a bifurcation of the equilibrium deformations, and is characteristic of the classical type of buckling, although other kinds of buckling may exhibit the same phenomenon. P_{cr} is defined as the classical buckling load for this structure, and is given by [1] as

$$P_{cr} = \frac{\pi^2 EI}{L^2}, \quad (1.1)$$

where E is Young's modulus of the elastic material, I the moment of inertia of the cross section (assumed independent of x), and L the column length.

If it is assumed that the column has some initial imperfection, which is a much more realistic approach than assuming a perfect column, then the load vs. lateral deflection parameter δ is given by the dashed curve $O'A'C'$ in Fig. 1.1c. Let $y_0(x)$ be a measure of the initial imperfection, then

$$y_0(x) = y(x) \quad \text{when } P = 0 . \quad (1.2)$$

As $y_0(x) \rightarrow 0$ the load deformation curve $O'A'C'$ approaches the curve OAC but never OAB ; thus for a non-perfect column the load deformation relation always has a unique one-to-one correspondence. There is no bifurcation point and no well defined buckling load. However, as can be seen from Fig. 1.1c, the classical buckling load P_{cr} of the perfect column serves a very useful purpose for the non-perfect column, in that as $P \rightarrow P_{cr}$ the ratio δ/δ_0 increases very rapidly. Thus P_{cr} may be considered as an upper limit of useful loads that can be supported by the non-perfect column. As will be shown, the same cannot be said about the critical buckling load of a perfect viscoelastic column, whose analysis follows.

Consider a centrally loaded straight viscoelastic column loaded as shown in Fig. 1.1a. If the column does not buckle, the only deformation is a shortening of the column due to the uniform axial load. If buckling is to take place, the lateral motion must be governed by the instantaneous modulus of the material since there is no motion in this direction before

buckling. Based on this the buckling load for a perfect viscoelastic column is

$$P_{cr} = \frac{\pi^2 E(0) I}{L^2} \quad (1.3)$$

where $E(0)$ is the instantaneous elastic modulus of the viscoelastic material, and is defined as the modulus governing the stress immediately after the material has been subjected to a suddenly applied strain.

If now a non-perfect viscoelastic column is considered, the lateral deflection is given as a function of time, initial imperfection, and load. The general features of the response of a non-perfect column to a load that is suddenly applied and then held constant can be brought out by a quasi-static linear analysis of a column whose initial imperfection consists of a lateral displacement in the form of a half sine wave.

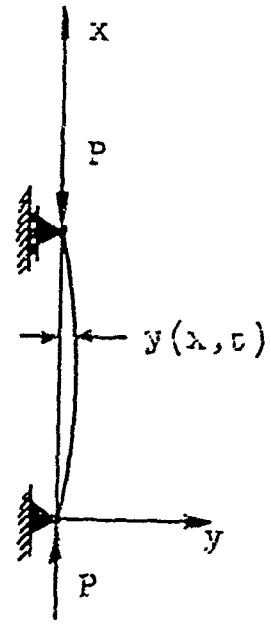
For the column as shown in Fig. 1.2a, let

$$y_0(x) = \delta_0 \sin \frac{\pi x}{L} \quad (1.4)$$

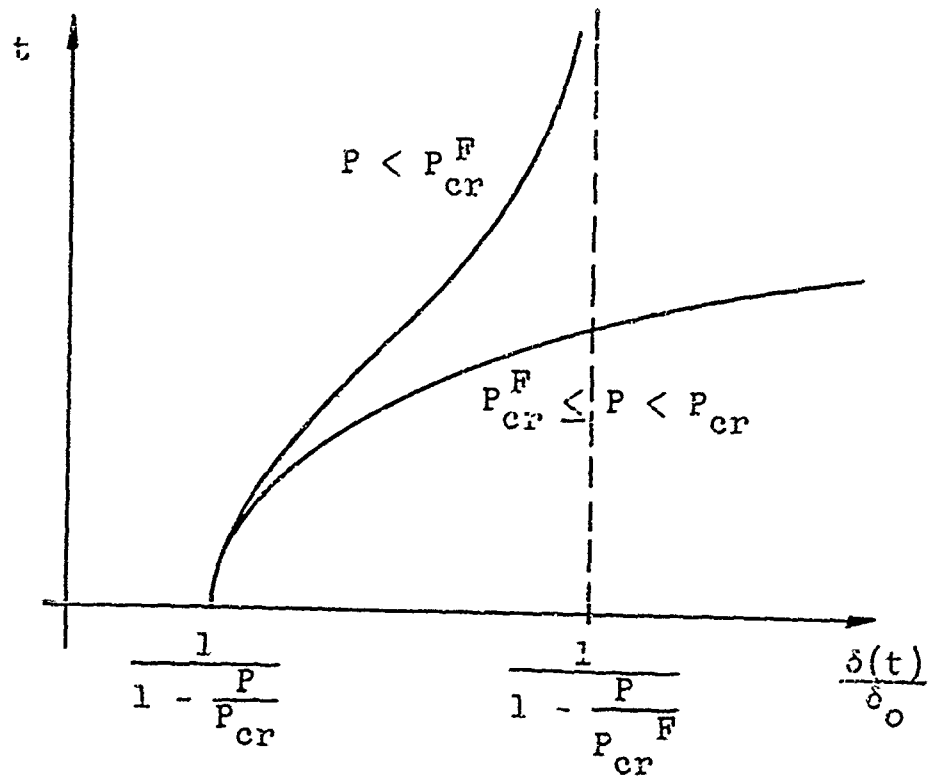
be the displacement before the load is applied, and

$$y(x,t) = \delta(t) \sin \frac{\pi x}{L} \quad (1.5)$$

the total displacement after loading.



(a)



(b)

Fig. 1.2

From the solution given in [2] for several different viscoelastic materials, it is seen that the displacement can be expressed as

$$y(x,t) = \frac{1}{1-P/P_{cr}} y_0(x) f(P,t) ,$$

or (1.6)

$$\delta(t) = \frac{1}{1-P/P_{cr}} \delta_0 f(P,t) ,$$

where P_{cr} is given by equation (1.3).

The function $f(P,t)$ represents the time response of the viscoelastic material. If for convenience we assume the load is applied at $t = 0$, then

$$f(P,0) = 1 , \quad (1.7)$$

and we have from equation (1.6)

$$y(x,0) = \frac{1}{1-P/P_{cr}} y_0(x) , \quad (1.8)$$

which is identical to the results for an elastic column analysis [1], using the same assumptions. It is obvious that as $P \rightarrow P_{cr}$ the displacement increases very rapidly, and thus P_{cr} is an upper limit on the loads that may be supported for a very short period of time.

The character of the function $f(P,t)$ depends very strongly on the load P . Let P_{cr}^F be defined as the long time critical load, which is given by

$$P_{cr}^F = \frac{\pi^2 E_F I}{L^2} , \quad (1.9)$$

where E_F is the long time or final modulus of the viscoelastic material, and is defined as the modulus governing the stress for an infinitely long time application of a constant strain. A viscoelastic fluid is characterized by having $E_F = 0$ while for a viscoelastic solid $0 < E_F \leq E(0)$. These properties are more fully described in Chapter 2.

For
$$P \geq P_{cr}^F, \quad f(P,t) \rightarrow \infty \quad \text{as } t \rightarrow \infty, \quad (1.10)$$

and for

$$P < P_{cr}^F, \quad f(P,t) \rightarrow \frac{1-P/P_{cr}}{1-P/P_{cr}^F} \quad \text{as } t \rightarrow \infty. \quad (1.11)$$

Thus it is seen that for loads $P \geq P_{cr}^F$, the column is essentially unstable as the deflection keeps increasing indefinitely, while for loads $P < P_{cr}^F$ the column is stable in the sense that the deflection remains finite. Fig. 1.2b shows a qualitative plot of the column deflection vs. time. The curve for $P < P_{cr}^F$ is asymptotic to the dashed line

$$\frac{\delta(t)}{\delta_0} = \frac{1}{1-P/P_{cr}^F} \quad \text{while for } P_{cr}^F \leq P < P_{cr} \quad \text{the dashed line}$$

has no significance whatsoever. It is apparent from Fig. 1.2b that loads in the range $P_{cr}^F \leq P < P_{cr}$ can be supported for a short time, but for long time loading it is necessary that $P < P_{cr}^F$.

Comparing then the results of the elastic and viscoelastic analysis, it is seen that the critical buckling load of a perfect column, P_{cr} , serves as an upper limit for

the safe load that can be supported by an elastic column, even if the column is not perfect. However, for the viscoelastic column, P_{cr} serves as an upper limit only for the perfect column and for very short duration loadings of the imperfect column. If the load is to be applied for a long time to a viscoelastic column, then even for an infinitesimally small imperfection it is necessary to restrict the load to be less than P_{cr}^F .

A major problem in describing the behavior of an imperfect viscoelastic column occurs because in the analysis there is no natural criterion with which to associate failure other than the fact that for some load conditions the displacements become infinite. However, the displacements approach infinity only as the time also approaches infinity, and so this does not provide a unique measure of the column response for different viscoelastic materials. Thus, in the sense of some natural criterion, a finite critical buckling or failure time does not exist for any value of the load below P_{cr} [4], [8].

The second kind of buckling to be considered is of the snap-through type as exhibited by a shallow pin ended arch of uniform cross-section, loaded as shown in Fig. 1.3a.

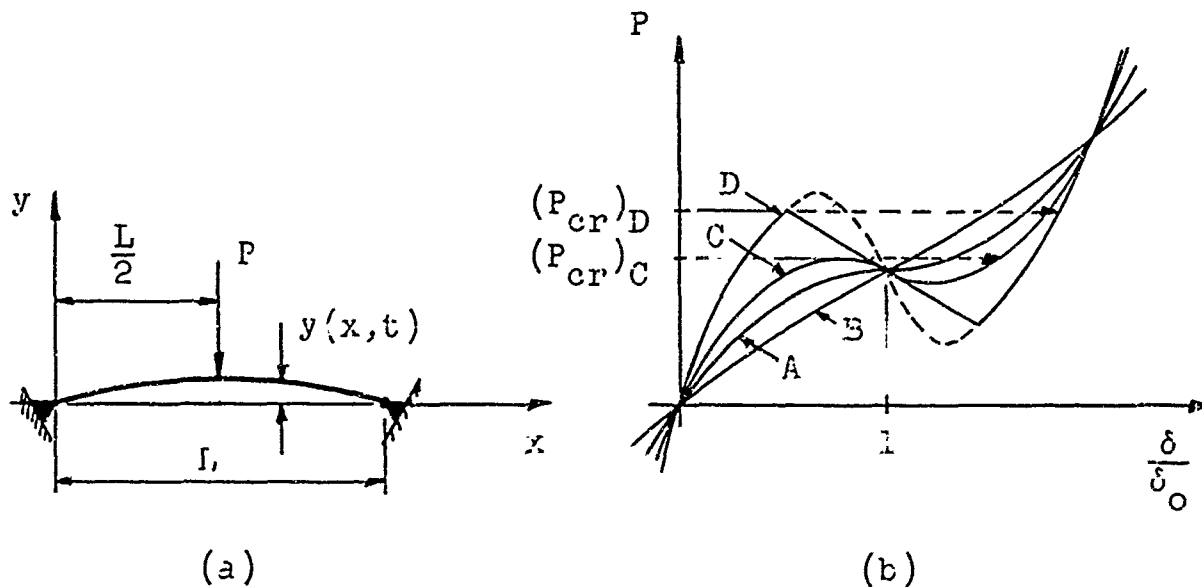


Fig. 1.3

In discussing the response of such an arch it is convenient to consider a loading consisting of only a concentrated load P as shown, although all the remarks carry through for distributed loads as well. The deflection of the midpoint of the arch under the load is designated by $\delta(t)$, thus

$$\left. \begin{aligned} \delta(t) &= y_0\left(\frac{L}{2}\right) - y\left(\frac{L}{2}, t\right) \\ &= \delta_0 - y\left(\frac{L}{2}, t\right) \end{aligned} \right\} \quad (1.12)$$

where $y_0(x)$ defines the initial unloaded shape of the arch, and

$$\delta_0 = y_0\left(\frac{L}{2}\right) \quad (1.13)$$

The load-deflection response of an elastic arch [11] is given in Fig. 1.3b. Curve A corresponds to an arch whose initial rise-to-span ratio, δ_0/L , is such that its load deflection curve has a horizontal tangent at the point

$\delta/\delta_0 = 1$, while curve B represents an arch whose initial rise-to-span ratio is less than that of the arch represented by A . For these two cases the load deflection relation has a one-to-one correspondence and there is no instability for any magnitude of the load. A physical explanation for this behavior is that because the arches are so shallow, the resistance to deformation by bending is much greater than that due to the axial thrust, and so the loss of the resistance by the axial thrust as the deflection increases is more than offset by the increase due to bending.

Curves C and D represent arches which are perfectly symmetrical with respect to the line $x = \frac{L}{2}$, and whose rise-to-span ratios are greater than those of A . In these cases there is a range of loading where the deflection is a multivalued function of the load, and so there is more than one equilibrium position for every value of P . For these cases then there is a well defined buckling load as shown by $(P_{cr})_C$ and $(P_{cr})_D$ in Fig. 1.3b, for at these loads the respective arches undergo a finite deformation, as shown by the dashed arrows, to a new stable equilibrium position.

Curve C represents an arch whose initial rise-to-span ratio is such that when the arch buckles, the deformations in going from the unbuckled to the buckled state are symmetrical, as shown in Fig. 1.4a. Curve D then represents an arch whose rise-to-span ratio is greater than C , and

which buckles unsymmetrically as shown in Fig. 1.4b.

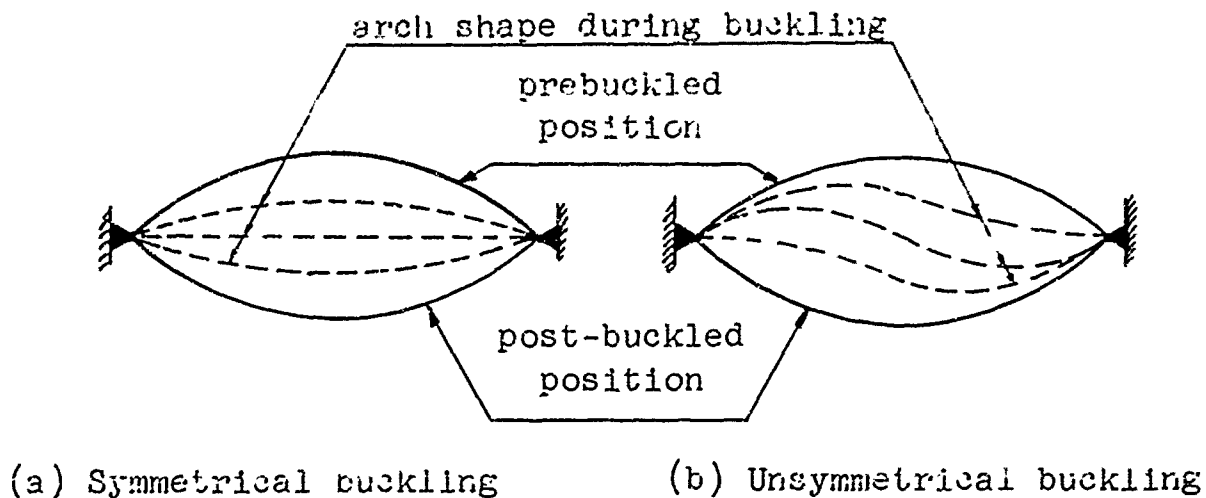


Fig. 1.4

The term snap-through can readily be seen to be a good description of this type of behavior, as the structure under a dead load would physically snap through to the post-buckled position.

For the case depicted by curve C the equilibrium deformation path (curve C) is seen to be a continuous curve with no bifurcation points. However, the equilibrium deformation path for case D consists of the curve D plus the dotted portion as shown in Fig. 1.3b. The dotted portion corresponds to symmetrical deformations, which are equilibrium deformations but are unstable. Thus at $P = (P_{cr})_D$ there is a bifurcation point, just as there was with the perfect column.

The load deformation curves for imperfect arches, that is, arches whose loading or initial shape is not symmetrical with respect to the line $x = \frac{L}{2}$, are shown in Fig. 1.5

with the dotted lines the corresponding curves for the symmetrical arches. (For discussion purposes here it is assumed that the non-symmetry is caused by the initial shape, and that this non-symmetry could be expressed by the second mode of a Fourier sine expansion of the initial arch shape.)

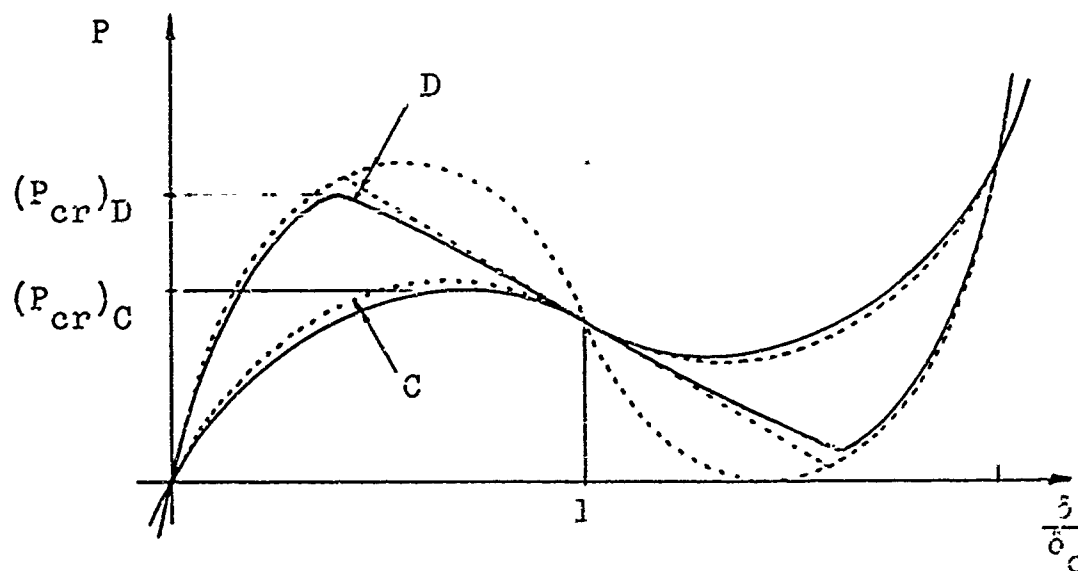


Fig. 1.5

The equilibrium deformation paths as shown are now all continuous with no bifurcation points, but there still exist well defined buckling loads $(P_{cr})_C$ and $(P_{cr})_D$. This is in contrast to the imperfect elastic column which has no well defined buckling load. Following the terminology in [17], unsymmetrical buckling at bifurcation points will be termed transitional buckling, in order to distinguish it from unsymmetrical buckling where there are no bifurcation points. Buckling where no bifurcation point is present will be termed non-transitional.

In this thesis a solution is given of the viscoelastic arch problem. It is found that the response of a viscoelastic arch is in many ways similar to an elastic arch. If the arch is very shallow then there is no instability; higher arches may buckle in either symmetrical or unsymmetrical modes, depending on the loading and the initial rise-to-span ratio. The main effect of the viscoelastic material is to permit the deformation to increase with time, even for a constant load P . This essentially decreases the stiffness of the arch in resisting additional load increments, and consequently decreases the buckling load. Thus it is possible for a constant load P to be stable at one time, but at some later time unstable.

In contrast to the response of a viscoelastic column, the viscoelastic arch buckles at a finite time if it buckles at all. For a sufficiently small load and a viscoelastic solid material the arch may always be stable, or it may be so shallow to begin with that instability does not occur. It is this latter case that most closely resembles the column response, since the arch deflections may keep on increasing indefinitely without buckling action if the viscoelastic material is of the fluid type. Another difference between the viscoelastic arch and column response is that for an imperfect arch whose non-symmetry is of infinitesimal magnitude, the buckling load and buckling time is different from the buckling load and buckling time of the corresponding

perfect arch only by an infinitesimal amount. It was seen earlier that for $P > P_{cr}^F$, the response of an imperfect viscoelastic column varied widely from the perfect column no matter what the magnitude of the imperfection.

The analysis as given in the main text is valid for an arbitrary initial arch shape (provided the arch is shallow), arbitrary lateral loading, and any linear viscoelastic material. Because numerical methods are required in the solution of the governing coupled non-linear integral equations, it is possible to use directly measured material properties in their numerical form.

The buckling criterion used in the solution is based on stability with respect to infinitesimal displacements about an equilibrium position. At any instant of time the response to an instantaneous displacement is governed by the initial modulus of the material, and so the stability can be investigated in the same general manner as the stability of an elastic arch, provided the time history of the deformation up to that instant is known. The theory also takes into account the possibility of buckling by the two different mechanisms, the transitional or non-transitional modes of failure.

The constitutive relations of the linear viscoelastic material are expressed in integral operator form (see Chapter 2) by the use of the relaxation modulus $E(t)$

$$\left(\sigma(t) = \int_{-\infty}^t E(t - t') \frac{d}{dt'} \epsilon(t') dt' \right), \text{ as opposed to the dif-}$$

ferential operator approach $\left(P\{\sigma(t)\} = Q\{\epsilon(t)\} \right)$, where P and Q are linear differential operators in t . For the arch problem, which is geometrically non-linear, the integral operator representation of the material offers several advantages over the more common differential operator representation. These advantages do not hold for the viscoelastic column problem since the column problem has a governing equation which is linear. The most widely accepted method of solving linear viscoelastic problems is by the use of the Laplace transform [13], and in the transform problem either representation of the material properties gives exactly the same result.

Some of the advantages of the use of integral operator relations in the arch problem and in general are:

- (a) the relaxation modulus can be measured directly by experiment.
- (b) the general form of the governing equations remains the same as for the elastic arch problem. This allows the same type of stability analysis and affords a good physical understanding of the viscoelastic effects.
- (c) the numerical integration is simplified. This is especially true if the material is quite complex, and would

require the use of high order differential operators if this approach were used.

Curves showing deformation vs. time for various load levels and buckling time vs. load are presented for two different materials. No attempt was made to give results for a wide number of situations; the examples were chosen so as to show the effect of some asymmetry in the structure or its loading, and to illustrate the basic difference in response between viscoelastic solid and fluid materials.

Arches made of viscoelastic solid materials may, if the load is small enough and constant as $t \rightarrow \infty$, approach a final stable equilibrium position. The equations governing the equilibrium position in this case reduce to the elastic equations with a modulus of elasticity of E_F ; these are algebraic equations and can be solved to find the final equilibrium position. The value of the final equilibrium position can then be used to evaluate the integrals in the equations that govern the buckling action, and this reduces these equations to algebraic equations. It is then possible to determine the additional load that would cause buckling at this time. Unfortunately the algebraic equations may be of quite high order and even for the simplest case the additional load cannot be expressed in explicit form. However, this method can be used to determine the instantaneous buckling load of an arch which has reached a final position without needing to know the entire relaxation function $E(t)$ of

the material or the time history of deformation. All that is required is the instantaneous modulus $E(0)$ and the final modulus E_F , which could actually be determined from the final position of the arch if this were known.

Results for this long time problem for several values of the final modulus and various loading conditions are given to compare the long time buckling load to the instantaneous or elastic buckling load.

Considerable work has been done on the so-called creep buckling of columns. Creep buckling is usually concerned with materials whose constitutive relations are non-linear, as opposed to the linear constitutive equations used in linear viscoelasticity. Most existing creep laws do not represent instantaneous and retarded elasticity as well as viscous flow which are all properties of linear viscoelasticity; however, for metals it is generally agreed that the non-linear creep laws give a better representation of the material behavior. Horf [16] gives a survey of the theories of creep buckling up to 1958.

Pian [10] has given an analysis for the creep buckling of a uniformly loaded arch using a 2-element non-linear Kelvin model to represent the material. By linearizing the model his problem reduces to the linear viscoelastic case. The Kelvin model is not a particularly good representation of material behavior, but because of its simplicity Pian is able to get a numerical solution for both the linear and non-linear

cases. However, his solution does not take into account the possibility of transitional buckling, and for cases where the transitional mode gives the critical buckling load or buckling time, Pian's results predict larger values.

Chapter II Linear Viscoelastic Materials

Viscoelastic materials are characterized by their property to deform with time under the action of a given loading. In a linear viscoelastic material, in particular, the constitutive relation is such that the ratio of stress to strain at any instant is a constant independent of the magnitude of the stress and strain.

In general two independent material functions are required to define completely a homogeneous, isotropic viscoelastic material in the same manner that two independent material constants are required to define a corresponding elastic material. However, in the work that follows only one material function need be considered because of the one-dimensional nature of the problem. For more general viscoelastic analysis see Bland [12] or Lee [13].

For this problem the most convenient formulation of the stress-strain relation is by the use of the relaxation modulus $E(t)$, which is defined by the relation

$$E(t) = \frac{\sigma(t)}{\epsilon_0}, \quad (2.1)$$

where $\sigma(t)$ is the stress resulting from an applied strain

$$\epsilon(t) = \epsilon_0 H(t) \quad (2.2)$$

$^1H(t)$ is the unit step function $H(t) = \begin{matrix} 0, & t < 0 \\ 1, & t \geq 0 \end{matrix}$

Since the material is considered linear this relation must hold for any value of ϵ_0 . $E(t) \equiv 0$ for $t < 0$ since the material is assumed to be undisturbed for $t < 0$.

The general form of $E(t)$ is the same for all materials. There is an initial discontinuity at $t = 0$, and the function then decreases monotonically to some final value, as shown in Fig. 2.1.

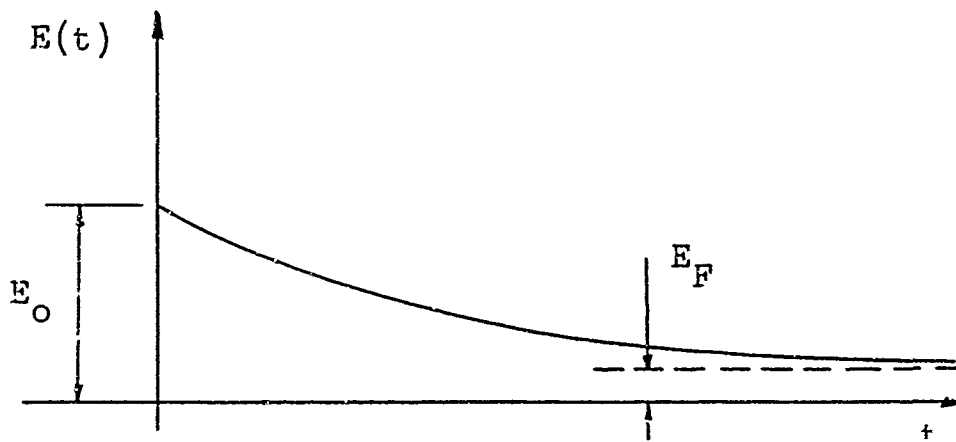


Fig. 2.1

The "initial modulus" of the material is defined as E_0 where $E_0 = E(0^+)$ ¹. Similarly the "final modulus" is defined as E_F where $E_F = \lim_{t \rightarrow \infty} E(t)$.

Linear viscoelastic materials fall into two general classifications, fluids and solids. For a fluid $E_F = 0$, whereas for a solid $E_F > 0$. A simple model representation

¹A variable written as t^+ refers to the value of this variable at $t + \epsilon$, and $t^- = t - \epsilon$, where ϵ is a positive infinitesimal quantity.

of a fluid is the Maxwell model, Fig. 2.2, in which a linear dashpot is connected in series to a linear spring.

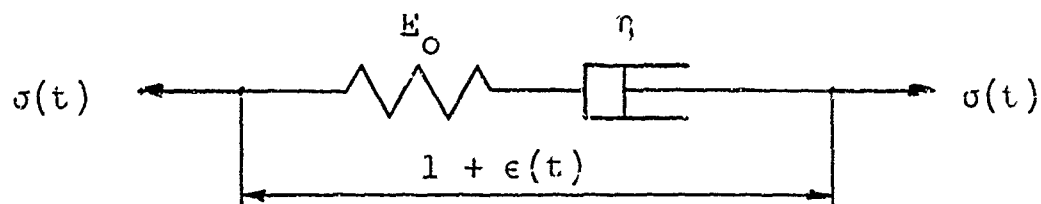


Fig. 2.2 Maxwell Fluid Model

Let t represent real time, then for the Maxwell fluid

$$E(t) = E_0 e^{-\frac{E_0}{\eta} t} \quad (2.3)$$

Define a dimensionless time parameter τ as

$$\tau = \frac{E_0}{\eta} t \quad , \quad (2.4)$$

and redefine the relaxation modulus as

$$E(\tau) = E_0 e^{-\tau} \quad (2.5)$$

$\frac{E_0}{\eta}$ is termed the relaxation time of the Maxwell material.

The simplest model representation of a solid material that exhibits an initial modulus is the three parameter solid of Fig. 2.3.

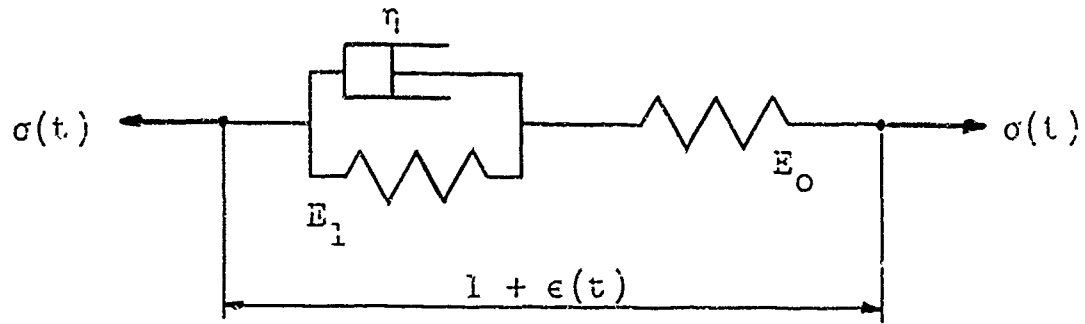


Fig. 2.3 Three Parameter Solid Model

For this model

$$E(t) = E_0 e^{-\frac{(E_1 + E_0)}{\eta} t} + \frac{E_1 E_0}{E_1 + E_0} \left(1 - e^{-\frac{(E_1 + E_0)}{\eta} t} \right). \quad (2.6)$$

The characteristic relaxation time is $\frac{E_1 + E_0}{\eta}$ and so

let

$$\tau = \frac{E_1 + E_0}{\eta} t. \quad (2.7)$$

The final modulus is clearly

$$E_F = \lim_{t \rightarrow \infty} E(t) = \frac{E_1 E_0}{E_1 + E_0} \quad (2.8)$$

In its most convenient form the relaxation modulus is then written as

$$E(\tau) = E_0 e^{-\tau} + E_F (1 - e^{-\tau}). \quad (2.9)$$

The essential difference in the model for a fluid or solid is that for a fluid there is at least one dashpot connected in series, whereas the dashpots in a solid material

are always connected in parallel with a spring.

In the work that follows the time parameter τ is always used. For real materials with measured relaxation properties, it is necessary to choose a characteristic relaxation time in order to define a dimensionless time parameter, but this can always be done. Lee and Rogers [14] discuss the use of measured material functions in stress analysis problems.

Since the stress-strain relations are linear the principle of superposition is valid and the stress for a smoothly varying strain can be represented by the integral

$$\sigma(\tau) = \int_{-\infty}^{\tau} E(\tau - \xi) \frac{d}{d\xi} \epsilon(\xi) d\xi \quad . \quad (2.10)$$

Such an integral is known as a Duhamel integral, and the kernel $E(\tau)$ is related to the Green's function of the differential operators that can alternately be used to express the stress-strain relations.

Chapter III General Analysis

Consider a shallow pin-ended arch of uniform cross-section loaded as shown in Fig. 3.1. The lateral load $q(x, \tau)$ always remains directed parallel to the y axis. Before the application of the lateral load the arch is considered to be unstrained and the location of its centroidal axis is given by $y_0(x)$. Under the action of the lateral load the centroidal axis will be displaced to a new position, and let this be denoted by $y(x, \tau)$. Without loss of generality we can assume $q(x, \tau) = 0$ for $\tau < 0$, and so

$$y(x, 0^-) = y_0(x) \quad (3.1)$$

becomes the initial condition for $y(x, \tau)$. $P(\tau)$ is the axial force induced in the arch by the end reactions and is directed as shown.

Assuming that $|y_0|$ and $|y|$ are much smaller than L , that the curvature remains small at all times so that $\left(\frac{\partial y(x, \tau)}{\partial x}\right)^2$ is negligible in comparison to 1, and that the thickness of the arch is much smaller than its radius of curvature; then the usual beam theory gives

$$\epsilon(x, \zeta, \tau) = \epsilon_0(\tau) - \zeta \left(\frac{\partial^2 y(x, \tau)}{\partial x^2} - \frac{d^2 y_0(x)}{dx^2} \right), \quad (3.2)$$

where $\epsilon(x, \zeta, \tau)$ is the strain of a longitudinal fibre of the arch located the distance ζ from the centroidal axis as shown in Fig. 3.2, and $\epsilon_0(\tau)$ is the strain of the centroidal axis which is assumed constant along the length of

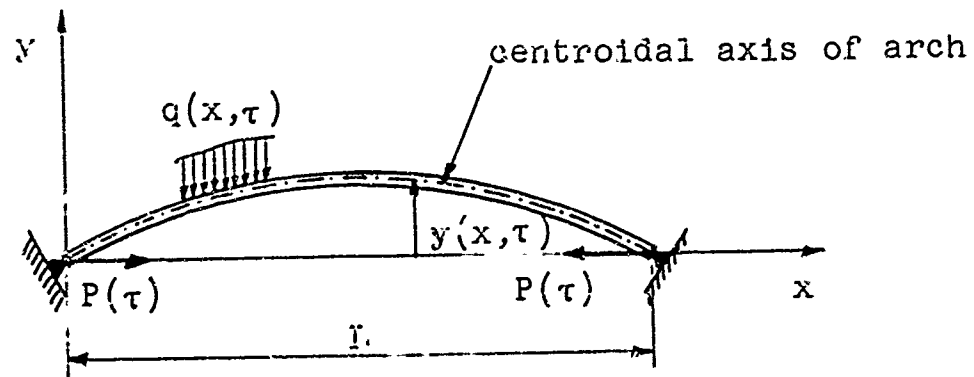


Fig. 3.1

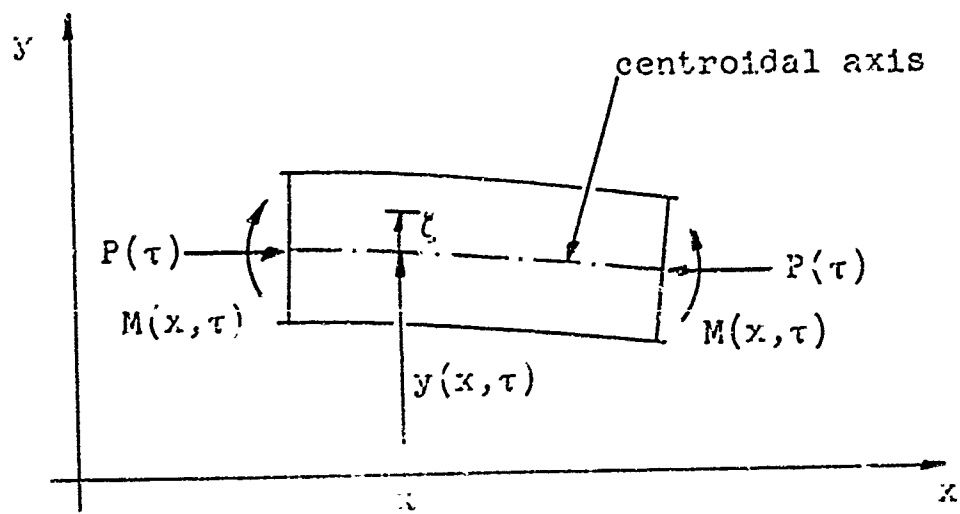


Fig. 3.2

the arch. This assumption relies on the fact that we are considering a shallow arch and that we also assume the axial force in the arch to be independent of x . The moment $M(x, \tau)$ as shown in Fig. 3.2 is given by

$$-M(x, \tau) = \iint_A \zeta \sigma(x, \zeta, \tau) dA, \quad (3.3)$$

where the negative sign is introduced to set up the sign convention that positive moment causes compressive stresses on the positive ζ side of the arch.

Now introduce the constitutive relation based on equation (2.10)

$$\sigma(x, \zeta, \tau) = \int_{0^-}^{\tau} E(\tau - \xi) \frac{\partial}{\partial \xi} \epsilon(x, \zeta, \xi) d\xi, \quad (3.4)$$

and substitute this into equation (3.3), which gives

$$-M(x, \tau) = \iint_A \zeta \int_{0^-}^{\tau} E(\tau - \xi) \frac{\partial}{\partial \xi} \epsilon(x, \zeta, \xi) d\xi dA. \quad (3.5)$$

Interchanging the order of integration and using equation (3.2) results in the moment-curvature relation

$$+M(x, \tau) = I \int_{0^-}^{\tau} E(\tau - \xi) \frac{\partial}{\partial \xi} \left(\frac{\partial^2 y(x, \xi)}{\partial x^2} \right) d\xi, \quad (3.6)$$

where $I = \iint_A \zeta^2 dA$, and $\iint_A \zeta dA = 0$

The moment-load relationship, using simple arch theory, is

$$\frac{\partial^2 M(x, \tau)}{\partial x^2} = - \frac{\partial^2}{\partial x^2} (P(\tau)y(x, \tau)) - q(x, \tau) \quad (3.7)$$

for the loads as directed in Fig. 3.1.

Since the arch supports are assumed rigid the projected length L of the arch must remain constant, thus

$$0 = - \epsilon_0(\tau) + \frac{1}{2L} \int_0^L \left\{ \left(\frac{\partial y(x, \tau)}{\partial x} \right)^2 - \left(\frac{dy_0(x)}{dx} \right)^2 \right\} dx \quad (3.8)$$

where the integral in the above expression is to a first approximation the change in projected length caused by the deflection.

The axial force $P(\tau)$ is given by

$$P(\tau) = - \iint_A \sigma(x, \zeta, \tau) dA$$

and by using equation (3.4) this becomes

$$P(\tau) = - \iint_A \int_0^{\tau} E(\tau - \xi) \frac{\partial}{\partial \xi} \epsilon(x, \zeta, \xi) d\xi dA \quad .$$

If the order of integration is interchanged and equation (3.2) is substituted into the resulting equation, it then yields

$$\begin{aligned} P(\tau) &= - \int_0^{\tau} E(\tau - \xi) \frac{\partial}{\partial \xi} \iint_A \left[\epsilon_0(\xi) - \zeta \left(\frac{\partial^2 y(x, \xi)}{\partial x^2} \right) \right] dA d\xi \\ &= - A \int_0^{\tau} E(\tau - \xi) \frac{d}{d\xi} \epsilon_0(\xi) d\xi \quad , \end{aligned} \quad (3.9)$$

since $A = \iint_A dA$. Now by using equation (3.8) we can express $P(\tau)$ in terms of the position of the arch; thus

$$P(\tau) = - \frac{A}{2L} \int_{0^-}^{\tau} E(\tau - \xi) \frac{\partial}{\partial \xi} \int_0^L \left(\frac{\partial y(x, \xi)}{\partial x} \right)^2 dx d\xi \quad (3.10)$$

If equation (3.6) is differentiated twice with respect to x and substituted into equation (3.7), we have

$$I \int_{0^-}^{\tau} E(\tau - \xi) \frac{\partial}{\partial \xi} \left(\frac{\partial^4 y(x, \xi)}{\partial x^4} \right) d\xi = - P(\tau) \frac{\partial^2 y(x, \tau)}{\partial x^2} - q(x, \tau) \quad .$$

By using equation (3.10), $P(\tau)$ in the above equation can be eliminated which results in

$$\begin{aligned} & - \frac{A}{2L} \frac{\partial^2 y(x, \tau)}{\partial x^2} \int_{0^-}^{\tau} E(\tau - \xi) \frac{\partial}{\partial \xi} \int_0^L \left(\frac{\partial y(x, \xi)}{\partial x} \right)^2 dx d\xi \\ & + I \int_{0^-}^{\tau} E(\tau - \xi) \frac{\partial}{\partial \xi} \left(\frac{\partial^4 y(x, \xi)}{\partial x^4} \right) d\xi = - q(x, \tau) \quad , \quad (3.11) \end{aligned}$$

the governing integro-differential equation for the arch.

The boundary conditions are

$$\begin{aligned} y(0, \tau) &= y(L, \tau) = 0 \\ \frac{\partial^2 y(0, \tau)}{\partial x^2} &= \frac{\partial^2 y(L, \tau)}{\partial x^2} = 0 \end{aligned} \quad (3.12)$$

and the initial condition is

$$y(x, 0^-) = y_0(x) \quad . \quad (3.13)$$

If $y_0(x)$ and $y(x, \tau)$ are expressed in a Fourier sine series, this will satisfy the boundary equations (3.12), and allow the space derivatives in equation (3.11) to be removed.

Thus let

$$y_0(x) = \sum_{m=1}^{\infty} a_m L \sin \frac{m\pi x}{L}, \quad (3.14)$$

and

$$y(x, \tau) = \sum_{m=1}^{\infty} b_m(\tau) L \sin \frac{m\pi x}{L}, \quad (3.15)$$

where a_m is a dimensionless constant and $b_m(\tau)$ is a dimensionless function of time.

It is convenient also to express the lateral load $q(x, \tau)$ in a Fourier sine series; thus

$$q(x, \tau) = q_0 \sum_{m=1}^{\infty} R_m(\tau) \sin \frac{m\pi x}{L}, \quad (3.16)$$

where $R_m(\tau)$ is a dimensionless function of time and q_0 is a constant having the same dimensions as $q(x, \tau)$.

Substituting equations (3.14), (3.15) and (3.16) into equation (3.11) gives

$$\frac{A}{2L} \left(\frac{\pi^2}{L} \sum_{m=1}^{\infty} m^2 b_m(\tau) \sin \frac{m\pi x}{L} \right) \int_{0^-}^{\tau} E(\tau - \xi) \frac{d}{d\xi} \left\{ \frac{\pi^2 L}{2} \sum_{k=1}^{\infty} k^2 b_k^2(\xi) \right\} d\xi$$

$$+ I \int_{0^-}^{\tau} E(\tau - \xi) \frac{d}{d\xi} \left\{ \frac{\pi^4}{L^3} \sum_{m=1}^{\infty} m^4 b_m(\xi) \sin \frac{m\pi x}{L} \right\} d\xi$$

$$= - q_0 \sum_{m=1}^{\infty} R_m(\tau) \sin \frac{m\pi x}{L}, \quad (3.17)$$

where

$$\int_0^L \left(\frac{\partial y(x, \xi)}{\partial x} \right)^2 dx = \int_0^L \left(\sum_{m=1}^{\infty} m\pi b_m(\tau) \cos \frac{m\pi x}{L} \right)^2 dx$$

$$= \frac{\pi^2 L}{2} \sum_{k=1}^{\infty} k^2 b_k^2(\tau)$$

because of the orthogonality property of the cosine functions.

Interchanging the order of integration and summation in the second term of equation (3.17), and rearranging results in

$$\sum_{m=1}^{\infty} \sin \frac{m\pi x}{L} \left\{ \frac{\pi^4 A}{4L} m^2 b_m(\tau) \int_{0^-}^{\tau} E(\tau - \xi) \frac{d}{d\xi} \left[\sum_{k=1}^{\infty} k^2 b_k^2(\xi) \right] d\xi \right.$$

$$\left. + \frac{\pi^4 I}{L^3} m^4 \int_{0^-}^{\tau} E(\tau - \xi) \frac{d}{d\xi} b_m(\xi) d\xi + q_0 R_m(\tau) \right\} = 0$$

Because the sine functions are orthogonal over the interval 0 to L each coefficient of $\sin \frac{m\pi x}{L}$ in the series must vanish, and so

$$m^2 \frac{\pi^4 A}{4L} b_m(\tau) \int_{0^-}^{\tau} E(\tau - \xi) \frac{d}{d\xi} \left[\sum_{k=1}^{\infty} k^2 b_k^2(\xi) \right] d\xi$$

$$+ m^4 \frac{\pi^4 I}{L^3} \int_{0^-}^{\tau} E(\tau - \xi) \frac{d}{d\xi} b_m(\xi) d\xi = - q_0 R_m(\tau) \quad (3.18)$$

$$m = 1, 2, 3 \dots$$

It is now convenient to introduce new notation to simplify the above equations. Let

$$A_m = \frac{L}{2} \sqrt{\frac{A}{I}} a_m, \quad B_m(\tau) = \frac{L}{2} \sqrt{\frac{A}{I}} b_m(\tau), \quad \text{and}$$

$$q_0 = \frac{2\pi^4 E_0 I}{L^4} \sqrt{\frac{I}{A}}.$$

Substituting these into equations (3.18) results in

$$\begin{aligned} m^2 \int_{0^-}^{\tau} \frac{E(\tau - \xi)}{E_0} \frac{d}{d\xi} B_m(\xi) d\xi + B_m(\tau) \int_{0^-}^{\tau} \frac{E(\tau - \xi)}{E_0} \frac{d}{d\xi} \sum_{k=1}^{\infty} k^2 B_k^2(\xi) d\xi \\ = - \frac{R_m(\tau)}{m^2} \quad m = 1, 2, 3 \dots \end{aligned} \quad (3.19)$$

with the initial conditions

$$B_m(0^-) = A_m, \quad m = 1, 2, 3 \dots \quad (3.20)$$

Here $E(\tau)$, $R_m(\tau)$ and A_m are known in the problem and it remains to find $B_m(\tau)$ and determine the stability of the arch.

The loading function $R_m(\tau)$ will normally be discontinuous at $\tau = 0$ (since $R_m(\tau) = 0$ for $\tau < 0$), and since we are assuming quasi-static response $B_m(\tau)$ will also be discontinuous at $\tau = 0$ as long as $E_0 \neq \infty$. It is convenient to remove this discontinuity at $\tau = 0$ by performing the integration in two steps, from 0^- to 0^+ and 0^+ to τ . Thus equations (3.19) become

$$\begin{aligned}
& m^2 \int_{0^+}^{\tau} \frac{E(\tau - \xi)}{E_0} \frac{d}{d\xi} B_m(\xi) d\xi + B_m(\tau) \int_{0^+}^{\tau} \frac{E(\tau - \xi)}{E_0} \frac{d}{d\xi} \sum_{k=1}^{\infty} k^2 B_k^2(\xi) d\xi \\
& + m^2 \frac{E(\tau)}{E_0} \left(B_m(0^+) - B_m(0^-) \right) \\
& + B_m(\tau) \frac{E(\tau)}{E_0} \left(\sum_{k=1}^{\infty} k^2 B_k^2(0^+) - \sum_{k=1}^{\infty} k^2 B_k^2(0^-) \right) \\
& = - \frac{R_m(\tau)}{m^2} \quad m = 1, 2, 3 \dots
\end{aligned}$$

Integrating the above integrals by parts, and by using the initial conditions as given by equations (3.20), yields

$$\begin{aligned}
B_m(\tau) & \left\{ m^2 + \sum_{k=1}^{\infty} k^2 \left(B_k^2(\tau) - A_k^2 \right) \right. \\
& \left. + \int_{0^+}^{\tau} \frac{E'(\tau - \xi)}{E_0} \sum_{k=1}^{\infty} k^2 \left(B_k^2(\xi) - A_k^2 \right) d\xi \right\} \\
& = - \frac{R_m(\tau)}{m^2} + m^2 A_m - m^2 \int_{0^+}^{\tau} \frac{E'(\tau - \xi)}{E_0} \left(B_m(\xi) - A_m \right) d\xi \\
& \quad m = 1, 2, 3 \dots \quad (3.21)
\end{aligned}$$

where the prime denotes differentiation with respect to the argument, i.e. $E'(\tau - \xi) = \frac{dE(\tau - \xi)}{d(\tau - \xi)}$.

At $\tau = 0^+$, equations (3.21) reduce to

$$B_m(0^+) \left\{ m^2 + \sum_{k=1}^{\infty} k^2 (B_k^2(0^+) - A_k^2) \right\} = - \frac{R_m(0^+)}{m^2} + m^2 A_m, \quad m = 1, 2, \dots \quad (3.22)$$

which correspond exactly to the equations of the purely elastic arch of modulus E_0 [11].

Equations (3.21) are an infinite system of coupled non-linear integral equations, and as such give very little encouragement for finding a closed-form solution. However, it is possible to integrate these equations numerically, since it will be shown that as long as the arch is stable any mode that is not excited, i.e. $A_m = R_m(\tau) = 0$, will have only the trivial solution $B_m(\tau) = 0$. Thus, as long as only a finite number of modes are excited, our system can be reduced to considering only this finite number plus one more.

To integrate equations (3.21) numerically, replace the time integrals with a step-by-step summation. Therefore, let $\tau_n = \tau$ ($\tau_0 = 0^+$) where n = the number of time steps required for the time to progress from 0^+ to τ .

Then

$$\int_{0^+}^{\tau} = \int_{\tau_0}^{\tau_n} = \sum_{i=0}^{n-1} \int_{\tau_i}^{\tau_{i+1}} = \sum_{i=0}^{n-2} \int_{\tau_i}^{\tau_{i+1}} + \int_{\tau_{n-1}}^{\tau_n}. \quad (3.23)$$

By using a simple trapezoidal approximation, the convolution type integrals we are concerned with can be expressed in the following form:

$$\int_{\tau_i}^{\tau_{i+1}} \frac{E'(\tau_n - \xi)}{E_0} f(\xi) d\xi \approx \left[\frac{E(\tau_n - \tau_i) - E(\tau_n - \tau_{i+1})}{E_0} \right] \left[\frac{f(\tau_i) + f(\tau_{i+1})}{2} \right] \quad (3.24)$$

Applying equations (3.23) and (3.24) to the first integral in equations (3.21), one gets

$$\begin{aligned} & \int_{0^+}^{\tau_n} \frac{E'(\tau - \xi)}{E_0} \sum_{k=1}^{\infty} k^2 (B_k^2(\xi) - A_k^2) d\xi \\ & \approx \frac{E(\tau_n - \tau_{n-1}) - E_0}{E_0} \left(\sum_{k=1}^{\infty} \frac{k^2 (B_k^2(\tau_{n-1}) + B_k^2(\tau_n) - 2A_k^2)}{2} \right) \\ & + \sum_{i=0}^{n-2} \frac{E(\tau_n - \tau_i) - E(\tau_n - \tau_{i+1})}{E_0} \left(\sum_{k=1}^{\infty} \frac{k^2 (B_k^2(\tau_i) + B_k^2(\tau_{i+1}) - 2A_k^2)}{2} \right) \\ & = E^*(\tau_n, \tau_{n-1}) \sum_{k=1}^{\infty} k^2 B_k^2(\tau_n) + S(\tau_n) \quad , \quad (3.25) \end{aligned}$$

where

$$E^*(\tau_n, \tau_{n-1}) = \frac{E(\tau_n - \tau_{n-1}) - E_0}{2E_0} \quad , \quad (3.26)$$

and

$$\begin{aligned}
S(\tau_n) &= E^*(\tau_n, \tau_{n-1}) \left(\sum_{k=1}^{\infty} k^2 (B_k^2(\tau_{n-1}) - 2A_k^2) \right) \\
&+ \sum_{i=0}^{n-2} \frac{E(\tau_n - \tau_i) - E(\tau_n - \tau_{i+1})}{2E_0} \left(\sum_{k=1}^{\infty} k^2 (B_k^2(\tau_i) + B_k^2(\tau_{i+1}) - 2A_k^2) \right).
\end{aligned}
\tag{3.27}$$

Similarly the second integral in equations (3.21) gives

$$\int_{0^+}^{\tau_n} \frac{E(\tau - \xi)}{E_0} (B_m(\xi) - A_m) d\xi = E^*(\tau_n, \tau_{n-1}) B_m(\tau_n) + S_m(\tau_n),
\tag{3.28}$$

where

$$\begin{aligned}
S_m(\tau_n) &= E^*(\tau_n, \tau_{n-1}) (B_m(\tau_{n-1}) - 2A_m) \\
&+ \sum_{i=1}^{n-2} \frac{E(\tau_n - \tau_i) - E(\tau_n - \tau_{i+1})}{2E_0} (B_m(\tau_i) + B_m(\tau_{i+1}) - 2A_m).
\end{aligned}
\tag{3.29}$$

Thus, by substituting equations (3.25) and (3.29) into equations (3.21), one obtains

$$\begin{aligned}
B_m(\tau_n) &\left\{ \left(1 + E^*(\tau_n, \tau_{n-1}) \right) \left(m^2 + \sum_{k=1}^{\infty} k^2 B_k^2(\tau_n) \right) - \sum_{k=1}^{\infty} k^2 A_k^2 + S(\tau_n) \right\} \\
&= - \frac{R_m(\tau_n)}{m^2} + m^2 A_m - m^2 S_m(\tau_n) \quad m = 1, 2, 3 \dots \tag{3.30}
\end{aligned}$$

For $n = 0$ ($\tau = 0^+$), equations (3.30) reduce to equations (3.22).

Assuming that the arch has been stable up to and including $\tau = \tau_{n-1}$, then at the next time step, $\tau = \tau_n$, $S_m(\tau_n)$ and $S(\tau_n)$ are known, since they contain only the previously determined values of $B_m(\tau_n)$. Thus $B_m(\tau_n)$ can be determined from the system of equations (3.30), and a check can be made of the stability of the arch at this time.

For demonstrative purposes, two different loading cases will be considered. The first is a sinusoidal arch with a sinusoidal load, i.e., $A_m = R_m(\tau) = 0$ for $m > 1$, so that only the first mode is excited; the second case will have an additional mode excited, i.e., one A_m or $R_m(\tau) \neq 0$ for $m > 1$, in addition to A_1 and $R_1(\tau) \neq 0$. The second case can then be generalized to include any number of excited modes.

Chapter IV Sinusoidal Arch under Sinusoidal Loading

Consider the simple case of a low sinusoidal arch subjected to a sinusoidal load distribution, then

$$y_0(x) = a_1 L \sin \frac{\pi x}{L} = A_1 2 \sqrt{\frac{I}{A}} \sin \frac{\pi x}{L} , \quad (4.1)$$

$$q(x,t) = q_0 R_1(\tau) \sin \frac{\pi x}{L} = R_1(\tau) \frac{2 \pi^4 E_0 I}{L^4} \sqrt{\frac{I}{A}} \sin \frac{\pi x}{L} .$$

Equations (3.30), the general equations of equilibrium, then reduce to

$$\left. \begin{aligned} B_1(\tau_n) \left[\left(1 + E^*(\tau_n, \tau_{n-1})\right) \left(1 + \sum_1^{\infty} k^2 B_k^2(\tau_n)\right) - A_1^2 + S(\tau_n) \right] &= - R_1(\tau_n) + A_1 - S_1(\tau_n) \\ B_2(\tau_n) \left[\left(1 + E^*(\tau_n, \tau_{n-1})\right) \left(4 + \sum_1^{\infty} k^2 B_k^2(\tau_n)\right) - A_1^2 + S(\tau_n) \right] &= - 4S_2(\tau_n) \\ \vdots & \\ B_m(\tau_n) \left[\left(1 + E^*(\tau_n, \tau_{n-1})\right) \left(m^2 + \sum_1^{\infty} k^2 B_k^2(\tau_n)\right) - A_1^2 + S(\tau_n) \right] &= - m^2 S_m(\tau_n) \quad \text{where } m = 2, 3, 4 \dots \end{aligned} \right\} (4.2)$$

and for $n = 0$ these then become

$$\left. \begin{aligned}
B_1(0^+) \left[1 + \sum_1^{\infty} k^2 B_k^2(0^+) - A_1^2 \right] &= -R_1(0^+) + A_1 \\
B_2(0^+) \left[4 + \sum_1^{\infty} k^2 B_k^2(0^+) - A_1^2 \right] &= 0 \\
\vdots & \\
B_m(0^+) \left[m^2 + \sum_1^{\infty} k^2 B_k^2(0^+) - A_1^2 \right] &= 0 \quad .
\end{aligned} \right\} (4.3)$$

Equations (4.3) correspond exactly to the elastic arch buckline problem and are discussed at length in [11]. One solution of the system would have

$$\left. \begin{aligned}
B_2(0^+) = B_3(0^+) = B_4(0^+) = \dots = 0 \\
B_1(0^+) \left[1 + B_1^2(0^+) - A_1^2 \right] &= -R_1(0^+) + A_1 \quad .
\end{aligned} \right\} (4.4)$$

The relation between $B_1(0^+)$ and $R_1(0^+)$ as given by equations (4.4) is plotted in Fig. 4.1.

Depending on the value of A_1 there are several possibilities. If $A_1 \leq 1$, the curve has a monotonic slope and so there exists a unique one-to-one relation between $B_1(0^+)$ and $R_1(0^+)$. Thus for any given loading there is only one equilibrium position and the system is stable. If $A_1 > 1$, then for $R_1(0^+)$ between the points b and c there exist three possible equilibrium positions. Assuming that $B_1(0^-) = A_1$ the stable equilibrium position of the arch is given by the portion ab of the curve, provided $R_1(0^+) < R_s(0^+)$.

If $R_1(0^+) > R_s(0^+)$ the only equilibrium position is along de . Thus it is apparent that, if the load is increased beyond $R_s(0^+)$ the arch snaps through from b to d and follows the de portion of the curve.

The portion bc of the curve represents unstable equilibrium positions, while along cd the positions are again stable; however since the arch starts at a the portion ab represents the stable unbuckled equilibrium positions, and hence the point b is the critical point at which buckling occurs.

$R_s(0^+)$, which is termed the non-transitional buckling load, can be determined by setting

$$\frac{dR_1(0^+)}{dB_1(0^+)} = 0, \quad \text{for} \quad \frac{d^2R_1(0^+)}{dB_1^2(0^+)} < 0 \quad (4.5)$$

which results in

$$R_s(0^+) = A_1 + \sqrt{\frac{4}{27}(A_1^2 - 1)^3} \quad A_1 > 1 \quad (4.6)$$

Now a second solution of the system of equations (4.3) could exist. If one $B_m(0^+)$ in addition to $B_1(0^+)$ is different from zero, then the only two equations of the set (4.3) not identically satisfied are

$$\begin{aligned} B_1(0^+) \left[1 + B_1^2(0^+) + m^2 B_m^2(0^+) - A_1^2 \right] &= -R_1(0^+) + A_1 \\ B_m(0^+) \left[m^2 + B_1^2(0^+) + m^2 B_m^2(0^+) - A_1^2 \right] &= 0 \end{aligned} \quad (4.7)$$

This solution leads to the transitional buckling load if $B_m(0+) \neq 0$ is found to be a valid solution. If it is not a valid solution, then the arch will buckle in a symmetrical mode and $R_s(0+)$ will be the buckling load.

Since it is assumed that $B_m(0+) \neq 0$ the second of equations (4.7) gives

$$m^2 + B_1^2(0+) + m^2 B_m^2(0+) - A_1^2 = 0 \quad (4.8)$$

At this point it is seen that only one $B_m(0+)$ in addition to $B_1(0+)$ can be non-zero. If it is also assumed that $B_n(0+) \neq 0$, $n \neq 1, m$ then it is necessary that

$$m^2 + B_1^2(0+) + m^2 B_m^2(0+) + n^2 B_n^2(0+) - A_1^2 = 0 \quad ,$$

and

$$n^2 + B_1^2(0+) + m^2 B_m^2(0+) + n^2 B_n^2(0+) - A_1^2 = 0 \quad .$$

This clearly is a contradiction since $n \neq m$ and so the assumption that $B_n(0+) \neq 0$ is incorrect.

Substituting equation (4.8) into the first equation of (4.7) results in

$$B_1(0+) = - \frac{R_1(0+) + A_1}{m^2 - 1} \quad , \quad (4.9)$$

and then by using this result in equation (4.8), one obtains

$$m^2 B_m^2(0+) = - m^2 + A_1^2 - \left(\frac{R_1(0+) - A_1}{m^2 - 1} \right)^2 \quad . \quad (4.10)$$

Equation (4.9) is plotted in Fig. 4.2a as the full line, where the dotted line is the same curve as that of Fig. 4.1. Equation (4.10) is plotted in Fig. 4.2b.

From Fig. 4.2b or equation (4.10) it is seen that $B_m(0^+)$ has a real, non-zero solution only in a definite range of $R_1(0^+)$, and for this solution to exist $B_1(0^+)$ must lie on the straight line segment $b'c'$ of Fig. 4.2a. For $B_m(0^+) = 0$ the solution for $B_1(0^+)$ lies on the dotted curve of Fig. 4.2a. Thus for $R_1(0^+) < R_u(0^+)$, $B_1(0^+)$ is given by the curve ab' , and $B_m(0^+) = 0$. For $R_1(0^+) = R_u(0^+)$ the arch will snap through to the point d' , with $B_1(0^+)$ following the path $b'c'd'$ and $B_m(0^+)$ following either of the closed paths $fghkf$ of Fig. 4.2b. When $B_1(0^+)$ is on the path $b'c'$, $B_m(0^+)$ is non-zero and the arch deflection is unsymmetrical.

Thus we conclude that $R_1(0^+) = R_u(0^+)$ is the critical transitional buckling load. The lowest possible value of $R_u(0^+)$ will occur when $m = 2$ is substituted into equation (4.9), and so the second mode will be the other non-zero mode during the unsymmetrical snapping-through action.

In order for the arch to buckle unsymmetrically or as we have defined it, transitional buckling, the point b' must lie on the portion ab of the dotted curve of Fig. 4.2a, otherwise b will be the critical point and the arch will buckle symmetrically. It is possible for b' to lie on that portion of the dotted curve that goes from b to the $R_1(0^+)$ axis.

If this is the case then $R_s(0^+)$ is the critical load but the deformation in going from b to d will be symmetrical from b to b' , unsymmetrical from b' to c' and symmetrical again along $c'd$. Since the critical load is not changed from the symmetrical, non-transitional buckling load, and since the buckling is initiated in the manner of symmetrical buckling, it will be considered as non-transitional in the remainder of this dissertation.

From equations (4.4) and (4.9) it is seen that if $A_1 \geq \sqrt{5.5}$, b' will fall on the portion ab and the critical load will be $R_1(0^+) = R_u(0^+)$. $R_u(0^+)$ is determined by setting $B_m(0^+) = 0$ in equation (4.10) which gives, for $m = 2$

$$R_u(0^+) = A_1 + 3\sqrt{A_1^2 - 4} \quad (4.11)$$

Thus the critical value of the loading is:

$$\begin{aligned} \left[R_1(0^+) \right]_{cr} = R_s(0^+) &= A_1 + \sqrt{\frac{4}{27}(A_1^2 - 1)^3} \\ &\text{for } 1 \leq A_1 \leq \sqrt{5.5} \end{aligned} \quad (4.12)$$

$$\begin{aligned} \left[R_1(0^+) \right]_{cr} = R_u(0^+) &= A_1 + 3\sqrt{A_1^2 - 4} \\ &\text{for } A_1 \geq \sqrt{5.5} . \end{aligned}$$

Now assuming that $R_1(0^+) < \left[R_1(0^+) \right]_{cr}$, i.e. the arch is stable at $\tau = 0^+$, $B_1(0^+)$ is given by the second of equations (4.4) and $B_m(0^+) = 0$, $m = 2, 3, 4, \dots$. Thus

the important conclusion is reached that, if the arch is stable, the sinusoidal configuration is maintained.

Proceeding on to the next time step $\tau = \tau_1$, it is now possible to calculate $J(\tau_1)$ and $S_m(\tau_1)$ since the values of $B_m(0^+)$ are known. Hence from equations (3.27) and (3.29) it is seen that $S(\tau_1)$ and $S_1(\tau_1)$ are non-zero, but that $S_m(\tau_1) = 0$, $m = 2, 3, 4 \dots$, since $B_1(0^+) \neq 0$, $B_m(0^+) = 0$ for $m = 2, 3, 4 \dots$.

Inserting these results in equations (4.2) gives, for $\tau_r = \tau_1$

$$B_1(\tau_1) \left[\left(1 + E^*(\tau_1, 0^+)\right) \left(1 + \sum_{k=1}^{\infty} k^2 B_k^2(\tau_1)\right) - A_1^2 + S(\tau_1) \right] = -R_1(\tau_1) + A_1 - S_1(\tau_1) \quad (4.13)$$

$$B_m(\tau_1) \left[\left(1 + E^*(\tau_1, 0^+)\right) \left(m^2 + \sum_{k=1}^{\infty} k^2 B_k^2(\tau_1)\right) - A_1^2 + S(\tau_1) \right] = 0$$

$m = 2, 3, 4 \dots$

Equations (4.13) can only be used to determine the stable equilibrium values of $B_m(\tau_1)$ under the assumption that the arch does not buckle unsymmetrically in a transitional mode, and provided that an unbuckled equilibrium position exists. Using the same argument as was used for $\tau = 0^+$, this requires that

$$R_1(\tau_1) < A_1 - S_1(\tau_1) + \sqrt{\frac{4}{27} \frac{[A_1^2 - S_1(\tau_1) - (1 + E^*(\tau_1, 0^+))]^3}{1 + E^*(\tau_1, 0^+)}} \quad (4.14)$$

If $R_1(\tau_1)$ does not satisfy this inequality, then the arch has become unstable sometime between $\tau = 0^+$ and $\tau = \tau_1$, and has snapped through to a buckled equilibrium position. However, if equation (4.14) is satisfied, the unbuckled equilibrium value of $B_1(\tau_1)$ is the largest root of equations (4.13) when $B_m(\tau_1) = 0$, $m = 2, 3, 4 \dots$.

Instantaneous changes in deformation are governed by the initial modulus E_0 ; equations (4.13) are not applicable to this type of response since they are valid only for a small step in a smoothly varying continuous change, and therefore they cannot be used to predict the stability of the arch with respect to the transitional buckling mode. They are valid in the non-transitional case since, to the accuracy of the numerical work, they give the equilibrium position and if no nearby equilibrium position exists, then the arch must have snapped through to its buckled position.

To determine if the arch is stable at $\tau = \tau_1$, it is then necessary to look at the instantaneous response of the arch at this time. This can be done by applying an additional load, say ΔR_1 , at $\tau = \tau_1$ and then investigating the stability at $\tau = \tau_1^+$ by considering the $B_m(\tau_1^+)$ vs. $(R_1(\tau_1) + \Delta R_1)$ relations. In order that this additional load not affect conditions at a later time it must be applied for an infinitesimal time only, and in this respect it can be considered as an imaginary or pseudo load used exclusively for the determination of stability.

Thus under the assumptions that the arch does not buckle unsymmetrically and that an unbuckled equilibrium position exists, $B_1(\tau_1)$ is found from equations (4.13). It is then possible to calculate $S(\tau_1^+)$ and $S_m(\tau_1^+)$ to be used in investigating the stability at $\tau = \tau_1^+$. By definition, see equation (3.28)

$$S_m(\tau_1^+) + E^*(\tau_1^+, \tau_1) B_m(\tau_1^+) = \int_{0^+}^{\tau_1^+} \frac{E'(\tau_1^+ - \xi)}{E_0} (B_m(\xi) - A_m) d\xi ,$$

however

$$E^*(\tau_1^+, \tau_1) = \frac{E(\tau_1^+ - \tau_1) - E_0}{2E_0} = \frac{E(0^+) - E_0}{2E_0} = 0 ,$$

and

$$\int_{0^+}^{\tau^+} (\dots) = \int_{0^+}^{\tau} (\dots)$$

for the integrands considered here. Thus

$$S_m(\tau_1^+) = \int_{0^+}^{\tau_1} \frac{E'(\tau - \xi)}{E_0} (B_m(\xi) - A_m) d\xi$$

and by using equation (3.28) again this can be written as

$$S_m(\tau_1^+) = S_m(\tau_1) + E^*(\tau_1, 0^+) B_m(\tau_1) .$$

A similar argument follows for $S(\tau_1^+)$ and so

$$\left. \begin{aligned}
 S(\tau_1^+) &= S(\tau_1) + E^*(\tau_1, 0^+) B_1^2(\tau_1) \\
 S_1(\tau_1^+) &= S_1(\tau_1) + E^*(\tau_1, 0^+) B_1(\tau_1) \\
 S_m(\tau_1^+) &= 0 \quad m = 2, 3, 4 \dots
 \end{aligned} \right\} (4.15)$$

Substituting equations (4.15) directly into equations (4.2), and noting the load at $\tau = \tau_1^+$ is $R_1(\tau_1) + \Delta R_1$ gives

$$\left. \begin{aligned}
 E_1(\tau_1^+) &\left[1 + \sum_{k=1}^{\infty} k^2 B_k^2(\tau_1^+) - A_1^2 + S(\tau_1^+) \right] \\
 &= - \left(R_1(\tau_1) + \Delta R_1 \right) + A_1 - S_1(\tau_1^+) \\
 B_m(\tau_1^+) &\left[m^2 + \sum_{k=1}^{\infty} k^2 B_k^2(\tau_1^+) - A_1^2 + S(\tau_1^+) \right] = 0
 \end{aligned} \right\} (4.16)$$

$$m = 2, 3, 4 \dots$$

Equations (3.30) would give the same result if it were considered that $\tau_n = \tau_1^+$, $\tau_{n-1} = \tau$. They have not been used since it is desired that $\tau_n - \tau_{n-1}$ be a finite time step, and it is convenient to write $\tau_n^+ - \tau_n$ as an infinitesimal step.

The investigation of equations (4.16) follows the general procedure used in looking at equations (4.3). Again two possible solutions exist and the load deflection relations are plotted in Figs. 4.3a and 4.3b.

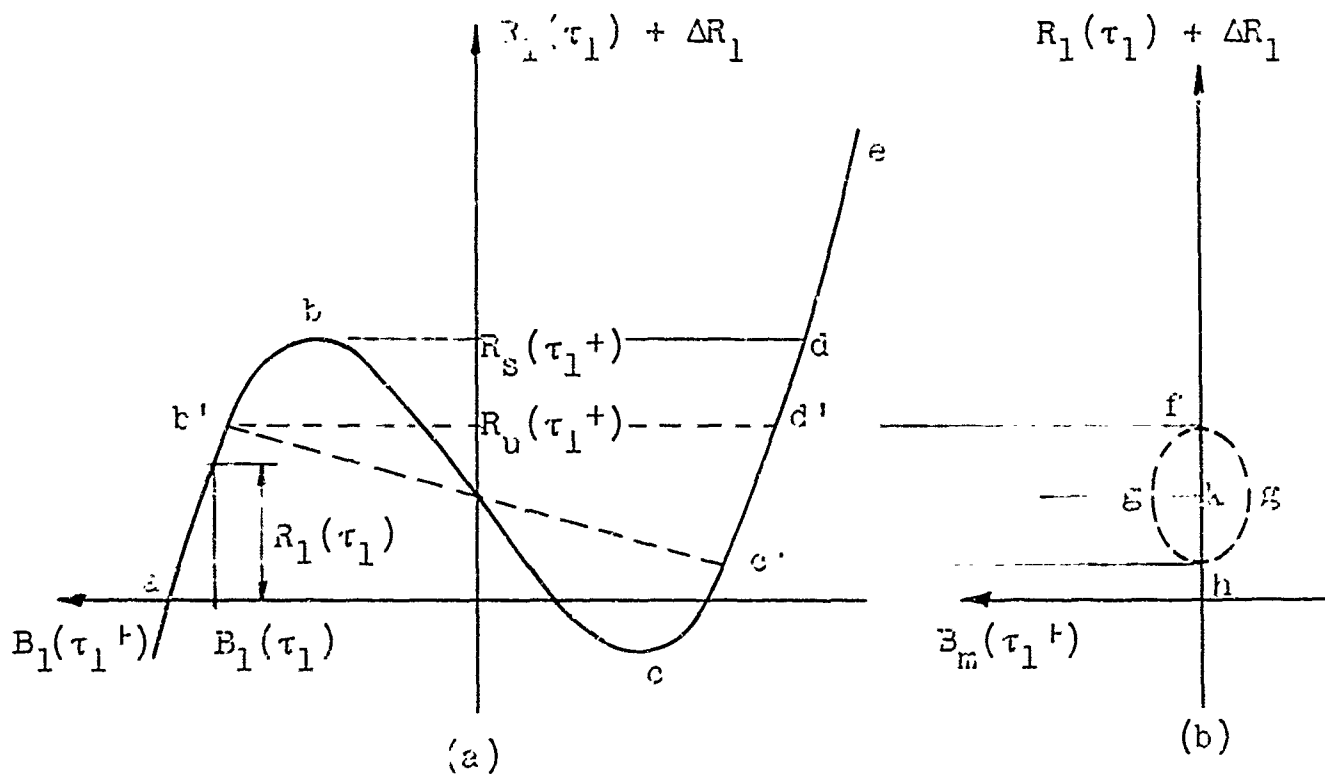


Fig. 4.3

The critical loads are given by

$$\begin{aligned}
 \left[R_1(\tau_1) + \Delta R_1 \right]_{cr} &= R_S(\tau_1^+) \\
 &= A_1 - S_1(\tau_1^+) + \sqrt{\frac{4}{27} (A_1^2 - S(\tau_1^+) - 1)^3} \\
 &\quad \text{for } 1 < A_1^2 - S(\tau_1^+) \leq 5.5
 \end{aligned}$$

and

$$\begin{aligned}
 \left[R_1(\tau_1) + \Delta R_1 \right]_{cr} &= R_U(\tau_1^+) \\
 &= A_1 - S_1(\tau_1^+) + 3\sqrt{A_1^2 - S(\tau_1^+) - 4} \\
 &\quad \text{for } A_1^2 - S(\tau_1^+) > 5.5
 \end{aligned}$$

(4.17)

If $R_u(\tau_1^+) < R_l(\tau_1) \leq R_s(\tau_1^+)$ then the assumption that the arch does not buckle unsymmetrically is incorrect, and the arch has become unstable sometime between $\tau = 0^+$ and $\tau = \tau_1$.

Thus if $R_l(\tau_1) < \left[R_l(\tau_1) + \Delta R_l \right]_{cr}$, the assumption made earlier regarding the existence of an unbuckled stable equilibrium position is valid, and the arch is stable under the load $R_l(\tau)$ up to and including $\tau = \tau_1$, for $R_l(\tau)$ monotonically increasing. If $R_l(\tau)$ is a decreasing function of time, there is a possibility of the arch becoming unstable between $\tau = 0^+$ and $\tau = \tau_1$ even if the analysis shows it to be stable at the two end times 0^+ and τ_1 . Thus special care must be taken in the choice of time steps to insure that this does not occur. Of course if the arch were stable at the time τ_1^+ for a loading $R_l(\tau_1) + \Delta R_l = R_l(0^+)$, then this would insure stability during the interval 0^+ to τ_1 .

Once stability is insured at $\tau = \tau_1$ it is possible to compute $S(\tau_2)$, $S_m(\tau_2)$ and proceed on to the second time step, where once again the same analysis can be made to determine the conditions at that time. This process can be repeated until the arch becomes unstable.

Fig. 4.4 shows the load deflection relation for a particular arch at several instants of time, and illustrates very clearly the effect of the creep on the response and buckling load of the arch as the time increases.

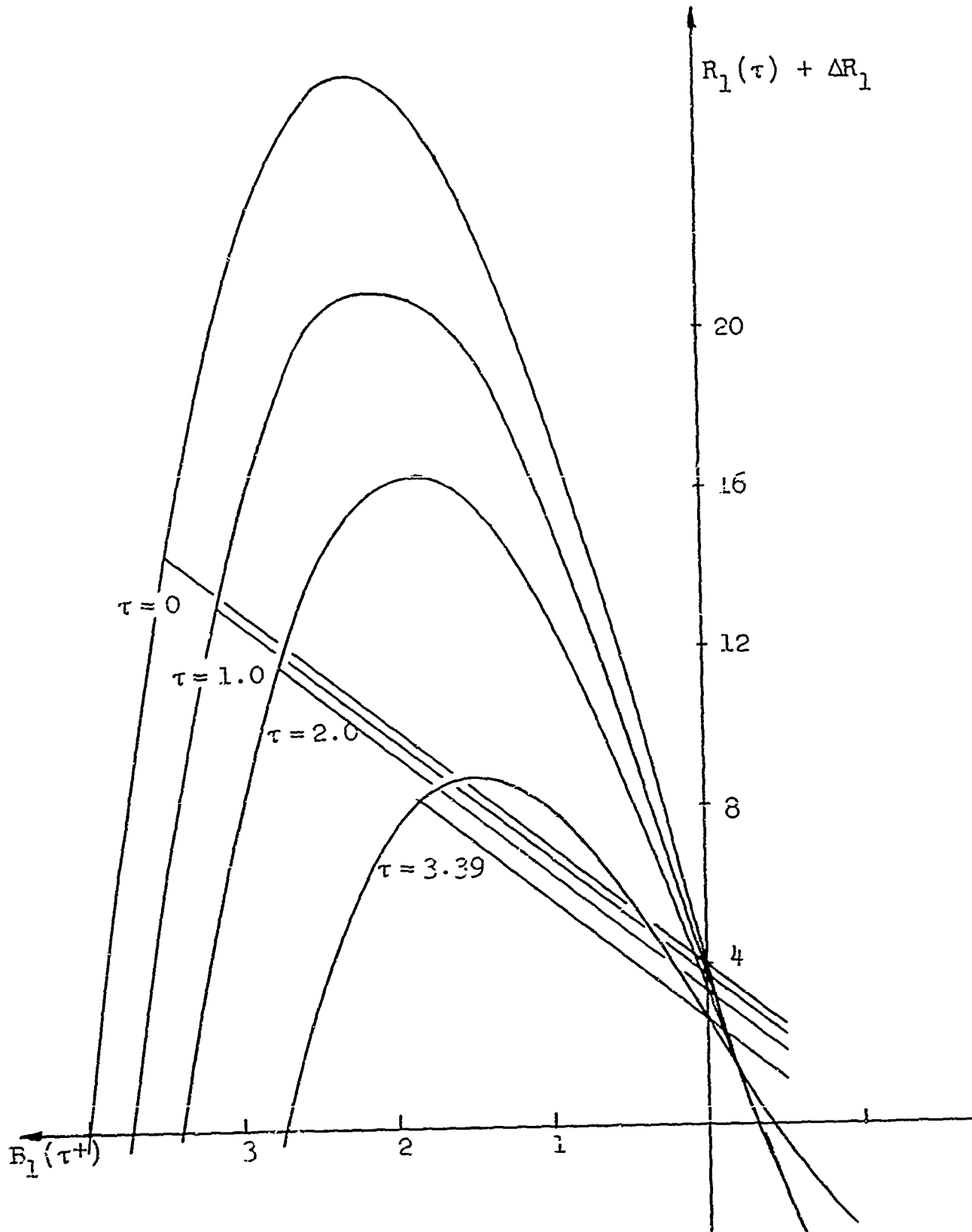


Fig. 4.4 Maxwell Fluid Material
 Sinusoidal Arch $A_1 = 4$
 Sinusoidal Load $R_1(\tau) = 8$

Chapter V Non-sinusoidal Arch

(V.I) Two modes excited

In the preceding chapter only the first mode $B_1(\tau)$ was excited, and it was shown that if the arch was stable, all other modes remained zero. Now consider an arch which has one additional mode excited, say, the r^{th} mode. This requires that A_r or $R_r(\tau)$ or both be non-zero.

Equations (3.30) then become

$$\left. \begin{aligned}
 & B_1(\tau_n) \left[(1 + E^*(\tau_n, \tau_{n-1})) \left(1 + \sum_{k=1}^{\infty} k^2 B_k^2(\tau_n) \right) \right. \\
 & \quad \left. - A_1^2 - r^2 A_r^2 + S(\tau_n) \right] = - R_1(\tau_n) + A_1 - S_1(\tau_n) \\
 & B_r(\tau_n) \left[(1 + E^*(\tau_n, \tau_{n-1})) \left(r^2 + \sum_{k=1}^{\infty} k^2 B_k^2(\tau_n) \right) \right. \\
 & \quad \left. - A_1^2 - r^2 A_r^2 + S(\tau_n) \right] = - \frac{R_r(\tau_n)}{r^2} + r^2 (A_r - S_r(\tau_n)) \\
 & \text{and} \\
 & B_m(\tau_n) \left[(1 + E^*(\tau_n, \tau_{n-1})) \left(m^2 + \sum_{k=1}^{\infty} k^2 B_k^2(\tau_n) \right) \right. \\
 & \quad \left. - A_1^2 - r^2 A_r^2 + S(\tau_n) \right] = - m^2 S_m(\tau_n)
 \end{aligned} \right\} (5.1)$$

where $m \neq 1, r$.

For $n = 0$ these reduce to

$$\begin{aligned}
B_1(0^+) \left[1 + \sum_{k=1}^{\infty} k^2 B_k^2(0^+) - A_1^2 - r^2 A_r^2 \right] &= -R_1(0^+) + A_1 \\
B_r(0^+) \left[r^2 + \sum_{k=1}^{\infty} k^2 B_k^2(0^+) - A_1^2 - r^2 A_r^2 \right] &= -\frac{R_1(0^+)}{r^2} + r^2 A_r \\
\vdots & \\
B_m(0^+) \left[m^2 + \sum_{k=1}^{\infty} k^2 B_k^2(0^+) - A_1^2 - r^2 A_r^2 \right] &= 0 .
\end{aligned} \quad \left. \vphantom{\begin{aligned} B_1(0^+) \\ B_r(0^+) \\ \vdots \\ B_m(0^+) \end{aligned}} \right\} (5.2)$$

In Chapter IV it was shown that as long as the arch is stable $S_m(\tau) = 0$, where m is an unexcited mode. Assuming that the same will hold true in this case and then proving that the assumption is correct allows equations (5.2) to be treated as a special case of equations (5.1) and so only one analysis is required. Thus setting $S_m(\tau_n) = 0$ in equations (5.1) gives

$$\begin{aligned}
B_1(\tau_n) \left[\left(1 + E^*(\tau_n, \tau_{n-1}) \right) \left(1 + \sum_{k=1}^{\infty} k^2 B_k^2(\tau_n) \right) \right. \\
\left. - A_1^2 - r^2 A_r^2 + S(\tau_n) \right] &= -R_1(\tau_n) + A_1 - S_1(\tau_n) \\
B_r(\tau_n) \left[\left(1 + E^*(\tau_n, \tau_{n-1}) \right) \left(r^2 + \sum_{k=1}^{\infty} k^2 B_k^2(\tau_n) \right) \right. \\
\left. - A_1^2 - r^2 A_r^2 + S(\tau_n) \right] &= -\frac{R_r(\tau_n)}{r^2} + r^2 (A_r - S_r(\tau_n)) \\
\vdots & \\
B_m(\tau_n) \left[\left(1 + E^*(\tau_n, \tau_{n-1}) \right) \left(m^2 + \sum_{k=1}^{\infty} k^2 B_k^2(\tau_n) \right) \right. \\
\left. - A_1^2 - r^2 A_r^2 + S(\tau_n) \right] &= 0 \quad m \neq 1, r .
\end{aligned} \quad \left. \vphantom{\begin{aligned} B_1(\tau_n) \\ B_r(\tau_n) \\ \vdots \\ B_m(\tau_n) \end{aligned}} \right\} (5.3)$$

As before, these equations should only be used to determine the unbuckled equilibrium values of $B_1(\tau_n)$ and $B_r(\tau_n)$ if they exist, under the assumption that $B_m(\tau_n) = 0$. The system can then be checked at $\tau = \tau_n$ to determine whether $B_m(\tau_n) = 0$ is a valid assumption under the loading $R_1(\tau_n)$ and $R_r(\tau_n)$.

The first two of equations (5.3) then become

$$B_1(\tau_n) \left[(1 + E^*(\tau_n, \tau_{n-1})) (1 + B_1^2(\tau_n) + r^2 B_r^2(\tau_n)) - A_1^2 - r^2 A_r^2 + S(\tau_n) \right] = -R_1(\tau_n) + A_1 - S_1(\tau_n) \quad (5.4a)$$

$$B_r(\tau_n) \left[(1 + E^*(\tau_n, \tau_{n-1})) (r^2 + B_1^2(\tau_n) + r^2 B_r^2(\tau_n)) - A_1^2 - r^2 A_r^2 + S(\tau_n) \right] = -\frac{R_r(\tau_n)}{r^2} + r^2 (A_r - S_r(\tau_n)) \quad (5.4b)$$

By maintaining the terms common to the two equations on the left, equations (5.4a) and (5.4b) yield

$$\begin{aligned} & (1 + E^*(\tau_n, \tau_{n-1})) (B_1^2(\tau_n) + r^2 B_r^2(\tau_n)) - A_1^2 - r^2 A_r^2 + S(\tau_n) \\ &= -\frac{R_1(\tau_n) + A_1 - S_1(\tau_n)}{B_1(\tau_n)} - (1 + E(\tau_n, \tau_{n-1})) \\ &= -\frac{\frac{R_r(\tau_n)}{r^2} + r^2 (A_r - S_r(\tau_n))}{B_r(\tau_n)} - (1 + E(\tau_n, \tau_{n-1})) r^2 \end{aligned}$$

Thus $B_r(\tau_n)$ can be expressed in terms of $R_1(\tau_n)$,

$$B_r(\tau_n) = \frac{\frac{-R_r(\tau_n)}{r^2} + r^2(A_r - S_r(\tau_n))}{\frac{-R_1(\tau_n) + A_1 - S_1(\tau_n)}{B_1(\tau_n)} + (r^2 - 1)(1 + E^*(\tau_n, \tau_{n-1}))} \quad (5.5)$$

Substituting this result back into equation (5.4a) to remove $B_r(\tau_n)$ gives

$$B_1(\tau_n) \left[(1 + E^*(\tau_n, \tau_{n-1})) \left\{ 1 + B_1^2(\tau_n) + r^2 \left(\frac{\left[-\frac{R_r(\tau_n)}{r^2} + r^2(A_r - S_r(\tau_n)) \right] B_1(\tau_n)}{-R_1(\tau_n) + A_1 - S_1(\tau_n) + (r^2 - 1)(1 + E^*(\tau_n, \tau_{n-1})) B_1(\tau_n)} \right)^2 \right\} - A_1^2 - r^2 A_r^2 + S(\tau_n) \right] = -R_1(\tau_n) + A_1 - S_1(\tau_n) \quad (5.6)$$

a fifth-order polynomial of $B_1(\tau_n)$.

Equation (5.6) is plotted in Fig. 5.1 as a function of $R_1(\tau_n)$, which assumes some functional dependence of $R_r(\tau_n)$ on $R_1(\tau_n)$. If $R_1(\tau_n) < \left[R_1(\tau_n) \right]_{cr}$ then an unbuckled equilibrium value exists under the assumptions made so far, and the stable $B_1(\tau_n)$ vs. $R_1(\tau_n)$ relation would be given by the curve ab of Fig. 5.1, which represents the largest root of equation (5.6). $B_r(\tau_n)$ can then be determined by substituting this value of $B_1(\tau_n)$ into equation (5.5).

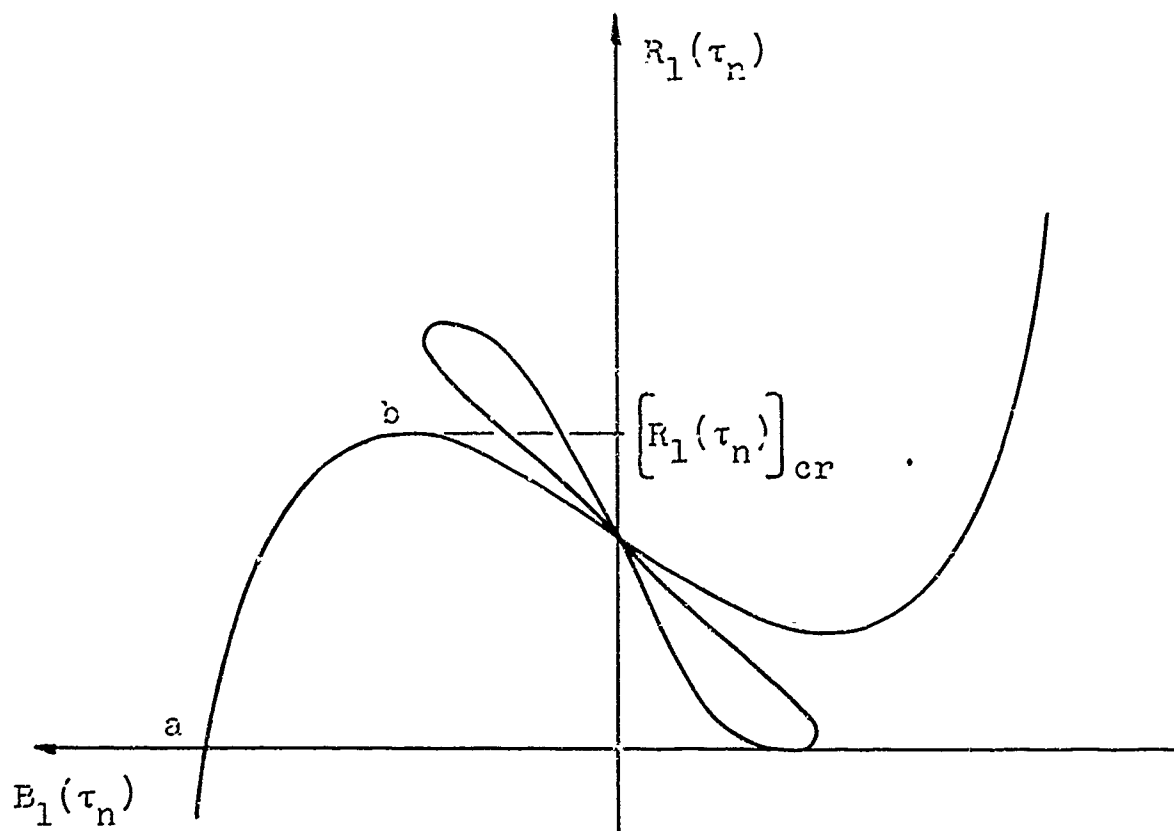


Fig. 5.1

It is now possible to calculate $S(\tau_n^+)$, $S_1(\tau_n^+)$, and $S_r(\tau_n^+)$; and it follows that $S_m(\tau_n^+) = 0$ since it was assumed that $B_m(\tau_n) = 0$. Thus following an argument similar to that used to derive equations (4.15) one gets

$$\begin{aligned}
S(\tau_n^+) &= S(\tau_n) + E^*(\tau_n, \tau_{n-1}) (B_1^2(\tau_n) + r^2 B_r^2(\tau_n)) \\
S_1(\tau_n^+) &= S_1(\tau_n) + E^*(\tau_n, \tau_{n-1}) B_1(\tau_n) \\
S_r(\tau_n^+) &= S_r(\tau_n) + E^*(\tau_n, \tau_{n-1}) B_r(\tau_n) \\
S_m(\tau_n^+) &= 0 \quad m \neq 1, r
\end{aligned}
\tag{5.7}$$

Substituting these results into equations (3.12), as was done before, and by noting that at $\tau = \tau_n^+$ it is desired to apply an additional load ΔR_1 and ΔR_r , it follows that

$$\begin{aligned}
& B_1(\tau_n^+) \left[1 + \sum_{k=1}^{\infty} k^2 B_k^2(\tau_n^+) - A_1^2 - r^2 A_r^2 + S(\tau_n^+) \right] \\
&= - (R_1(\tau_n) + \Delta R_1) + A_1 - S_1(\tau_n^+) \\
& B_r(\tau_n^+) \left[r^2 + \sum_{k=1}^{\infty} k^2 B_k^2(\tau_n^+) - A_1^2 - r^2 A_r^2 + S(\tau_n^+) \right] \\
&= - \frac{(R_r(\tau_n) + \Delta R_r)}{r^2} + r^2 (A_r - S_r(\tau_n^+)) \\
& \vdots \\
& B_m(\tau_n^+) \left[m^2 + \sum_{k=1}^{\infty} k^2 B_k^2(\tau_n^+) - A_1^2 - r^2 A_r^2 + S(\tau_n^+) \right] = 0 \\
& \quad m \neq 1, r
\end{aligned}
\tag{5.8}$$

It is convenient to consider ΔR_r as a function of ΔR_1 so that stability may be discussed with ΔR_1 the lone independent loading parameter. While this may not always be

desirable, it seems a reasonable assumption to make at this point.

In the investigation of the system of equations (5.8) there are again two possible solutions to consider. The first will be to assume $B_m(\tau_n^+) = 0$, which allows the first two of equations (5.8) to be rewritten so:

$$B_1(\tau_n^+) \left[1 + B_1^2(\tau_n^+) + r^2 \left(\frac{-\left(\frac{R_r(\tau_n) + \Delta R_r}{r^2} + r^2(A_r - S_r(\tau_n^+))\right) B_1(\tau_n^+)}{-\left(R_1(\tau_n) + \Delta R_1\right) + A_1 - S_1(\tau_n^+) + (r^2 - 1)B_1(\tau_n^+)} \right)^2 - A_1^2 - r^2 A_r^2 + S(\tau_n^+) \right] = -\left(R_1(\tau_n) + \Delta R_1\right) + A_1 - S_1(\tau_n^+) , \quad (5.9)$$

and

$$B_r(\tau_n^+) = \frac{-\left(\frac{R_r(\tau_n) + \Delta R_r}{r^2} + r^2(A_r - S_r(\tau_n^+))\right)}{\frac{-\left(R_1(\tau_n) + \Delta R_1\right) + A_1 - S_1(\tau_n^+)}{B_1(\tau_n^+) + (r^2 - 1)}} . \quad (5.10)$$

Equations (5.9) and (5.10) are plotted as the full lines on Figs. 5.2a and 5.2b respectively.

The broken line cr in Fig. 5.2a is given by

$$B_1(\tau_n^+) = \frac{-\left(R_1(\tau_n) + \Delta R_1\right) + A_1 - S_1(\tau_n)}{1 - r^2} , \quad (5.11)$$

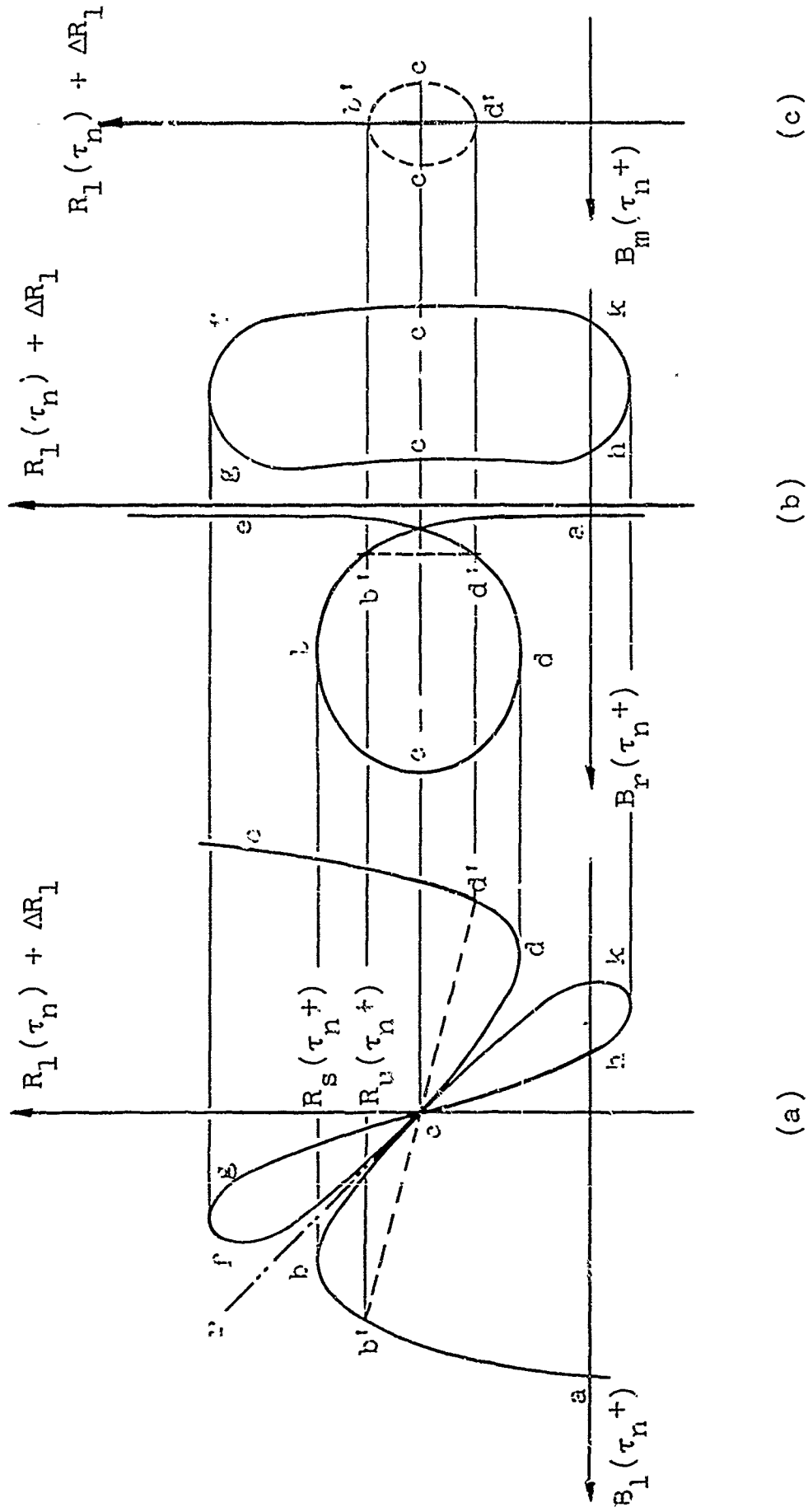


Fig. 5.2

which is found by setting the denominator of equation (5.10) equal to zero. It can be seen from equation (5.9) that no solutions of $B_1(\tau_n^+)$ will fall on this line except at the singular point c , and thus all possible stable equilibrium values fall below this line on the curve ab . Thus it is concluded that $R_1(\tau_n) + \Delta R_1 = R_s(\tau_n^+)$ is the non-transitional buckling load. $[R_1(\tau_n)]_{cr}$ as shown on Fig. 5.1 and $R_s(\tau_n^+)$ on Fig. 5.2a are equal only if $R_1(\tau_n) = [R_1(\tau_n)]_{cr}$. If the system is to have an unbuckled equilibrium value at $\tau = \tau_n$ then it is necessary that

$$R_1(\tau_n) < [R_1(\tau_n)]_{cr} < R_s(\tau_n^+) .$$

The other possible solution to the system of equations (5.8) has one value of $B_m(\tau_n^+) \neq 0$, $m \neq 1, r$. Thus the third of equations (5.8) gives

$$m^2 + B_1^2(\tau_n^+) + r^2 B_r^2(\tau_n^+) + m^2 B_m^2(\tau_n^+) - A_1^2 - r^2 A_r^2 + S(\tau_n^+) = 0 . \quad (5.12)$$

With the use of equation (5.12) the first two of equations (5.8) become

$$B_1(\tau_n^+) = \frac{-\left(R_1(\tau_n) + \Delta R_1\right) + A_1 - S_1(\tau_n^+)}{1 - m^2} , \quad (5.13)$$

and

$$B_r(\tau_n^+) = \frac{\frac{\left(R_r(\tau_n) + \Delta R_r\right)}{r^2} + r^2 \left(A_r - S_r(\tau_n^+)\right)}{r^2 - m^2} . \quad (5.14)$$

Substituting these two back into equation (5.12) results in

$$\begin{aligned}
 & m^2 B_m^2(\tau_n) \\
 &= -m^2 + A_1^2 + r^2 A_r^2 - S(\tau_n^+) - \left(\frac{-(R_1(\tau_n) + \Delta R_1) + A_1 - S_1(\tau_n)}{1 - m^2} \right)^2 \\
 &\quad - r^2 \left(\frac{\frac{-(R_r(\tau_n) + \Delta R_r)}{r^2} + r^2 (A_r - S_r(\tau_n^+))}{r^2 - m^2} \right)^2. \tag{5.15}
 \end{aligned}$$

If $r = 2$, $m > 2$ and so the line given by equation (5.13) would not intersect the curved segment ab of Fig. 5.2a, since its slope is greater than that of the line cr . Thus it can be concluded that, if $r = 2$, $B_m(\tau_n^+) \neq 0$ is not a possible solution and the mode of buckling will be non-transitional (i.e. no unexcited mode will be present in the collapse configuration).

If $r \geq 3$, then m may take on a value less than r and it may be possible to get a solution where $B_m(\tau_n^+) \neq 0$ is valid. Equations (5.13), (5.14) and (5.15) are plotted as the dashed lines on Figs. 5.2a, 5.2b, and 5.2c respectively, on the basis of $r \geq 3$ and $m < r$.

As was the case for the sinusoidal arch with sinusoidal load, if b' falls on the arc ab then the critical loading is $R_u(\tau_n^+)$, and by inspection of equation (5.13) it is seen that $m = 2$ would give the lowest value of $R_u(\tau_n^+)$. Unlike the sinusoidal case though, it is not convenient to give $R_s(\tau_n^+)$ and $R_u(\tau_n^+)$ in explicit form, since this

involves the solution of a fourth order polynomial rather than a second.

The conclusions to be drawn are:

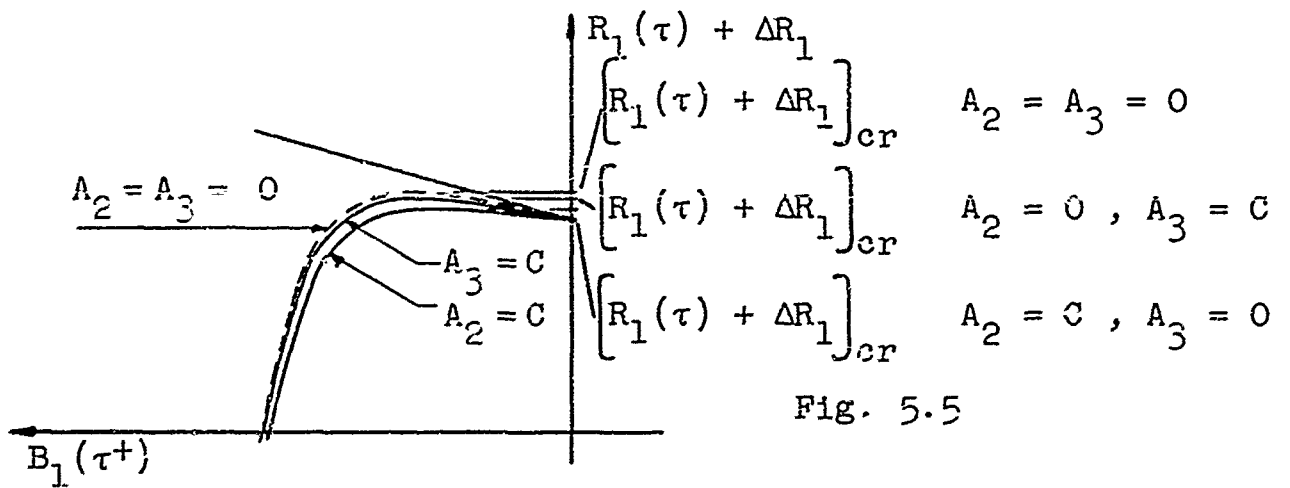
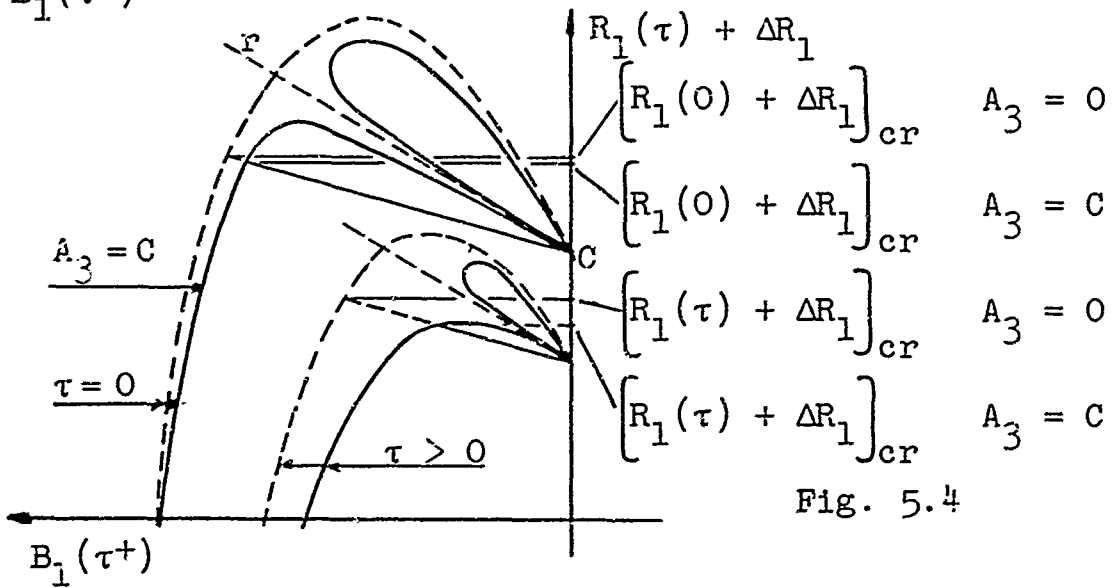
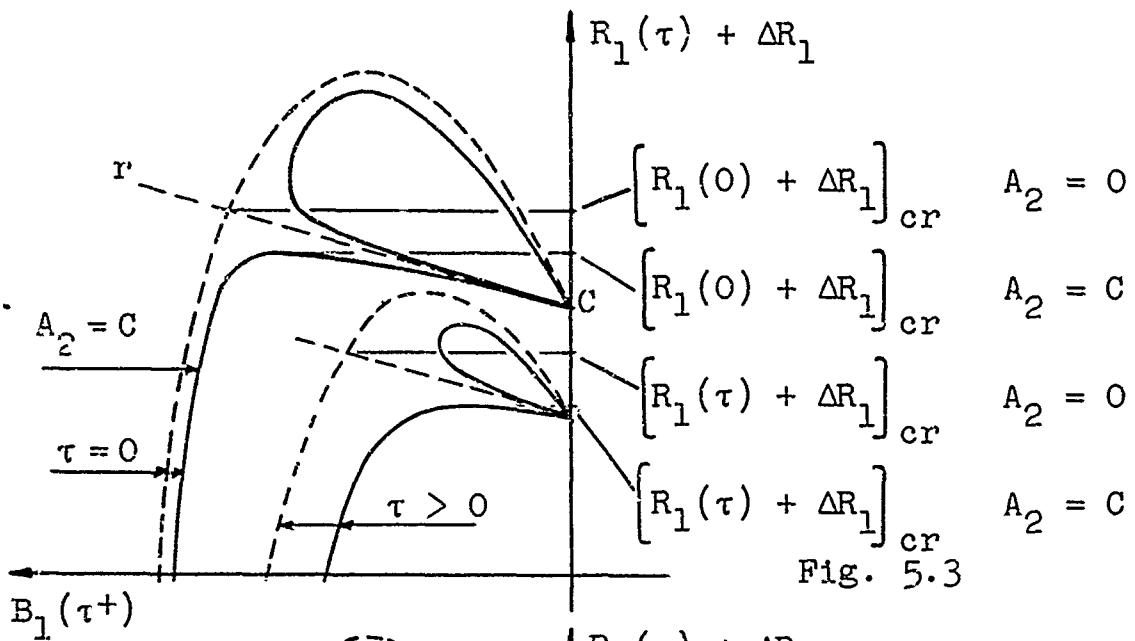
1. If $R_l(\tau_n) < R_s(\tau_n^+)$ or $R_u(\tau_n^+)$, whichever is smaller, then the arch is stable at $\tau = \tau_n$. Thus $B_l(\tau_n)$ and $B_r(\tau_n)$ found from equations (5.4a) and (5.4b), with $B_m(\tau_n) = 0$, are the stable equilibrium values.

2. Since $B_m(\tau_n) = 0$ as long as the arch is stable, $S_m(\tau_n) = 0$, and the assumption made at the beginning of the chapter that this is so is then proven to be valid.

3. If the second mode is excited, then any higher mode not excited remains zero for all time, stable or unstable.

It is interesting to note the influence of an excited nonsinusoidal mode upon the buckling load. If the second mode is the one that is excited, then a very small amount of asymmetry in the arch considerably lowers the critical load. Fig. 5.3 shows a typical load deflection relation at two different times, the dotted curve represents a sinusoidal arch while the full lines correspond to the same arch except that the second mode has been excited. It can be seen that there is considerable difference in the critical load for the two cases, and that the influence of this nonsinusoidal excitation increases with time.

Fig. 5.4 shows the response of the same basic arch as in Fig. 5.3 except that this case has the third mode excited instead of the second.



From Figs. 5.3 and 5.4 it can be seen that the effect of exciting the second mode on the buckling load of the arch is much greater than exciting the third mode. It can also be shown that exciting higher modes, either odd or even, does not have as much effect as exciting the second mode.

As the magnitude of the nonsinusoidal excitation decreases, the load deflection curves approach the dotted curve of the sinusoidal arch and the τ_{cr} line. Thus in the limit as the excitation goes to zero, the critical load for the nonsinusoidal arch approaches the critical load for the sinusoidal arch, as would be expected.

Figs. 5.3 and 5.4 correspond to arches that have an initial rise-to-span ratio such that the mode of buckling is transitional, which requires that $A_1^2 - S_1(\tau_{cr}^+) > 5.5$, where τ_{cr} is the time at which the arch buckles. If $A_1^2 - S_1(\tau_{cr}^+) < 5.5$, the sinusoidal arch will buckle in a nontransitional manner. Fig. 5.5 shows the response of such an arch with higher modes excited.

It can be seen from Fig. 5.5 that, for $A_2 = A_3$, the effect of the second mode being excited is again larger than the effect due to the third mode.

Comparison of Figs. 5.3 and 5.4 with 5.5 show that for $\frac{A_2}{A_1} = \frac{A_3}{A_1} = \text{constant}$, the influence of the nonsinusoidal mode on the buckling load decreases as A_1 decreases. For the elastic case [11] shows plots of critical load vs. A_1 for

various ratios of $\frac{A_2}{A_1}$ and $\frac{A_3}{A_1}$, and these show the above mentioned trend very clearly.

(V.II) Several modes excited

The solution of the problem is which many modes are excited, through either the initial arch shape or the loading, is a simple extension of the case of two modes excited.

Equations (5.1) through (5.5) remain valid except that r now stands for any excited mode except the first mode.

Equations (5.6) can then be written as

$$B_1(\tau_n) \left[\left(1 + E^*(\tau_n, \tau_{n-1}) \right) \left\{ 1 + B_1^2(\tau_n) + \sum_{k=r}^n k^2 \left(\frac{-R_k(\tau_n)}{k^2} + k^2(A_k - S_k(\tau_n)) \right) B_1(\tau_n) \right\} \right. \\ \left. - A_1^2 - \sum_{k=r}^n k^2 A_k^2 + S(\tau_n) \right] = -R_1(\tau_n) + A_1 - S_1(\tau_n), \quad (5.16)$$

a polynomial of $B_1(\tau_n)$ of order $(2h + 1)$, where n is the total number of excited modes.

Equation (5.16) is plotted in Fig. 5.5. The dashed curve in Fig. 5.6 is given by

$$B_1(\tau_n) \left[\left(1 + E^*(\tau_n, \tau_{n-1}) \right) \left(1 + B_1^2(\tau_n) \right) - A_1^2 - \sum_{k=r}^n k^2 A_k^2 + S(\tau_n) \right] \\ = -R_1(\tau_n) + A_1 - S_1(\tau_n),$$

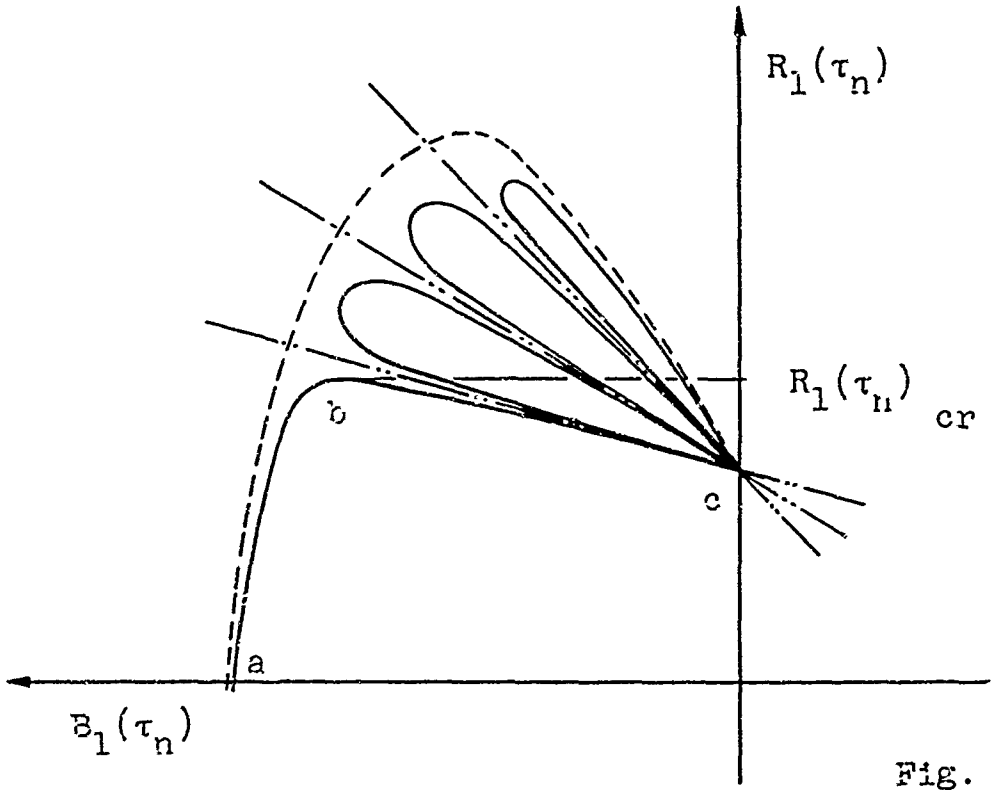


Fig. 5.6

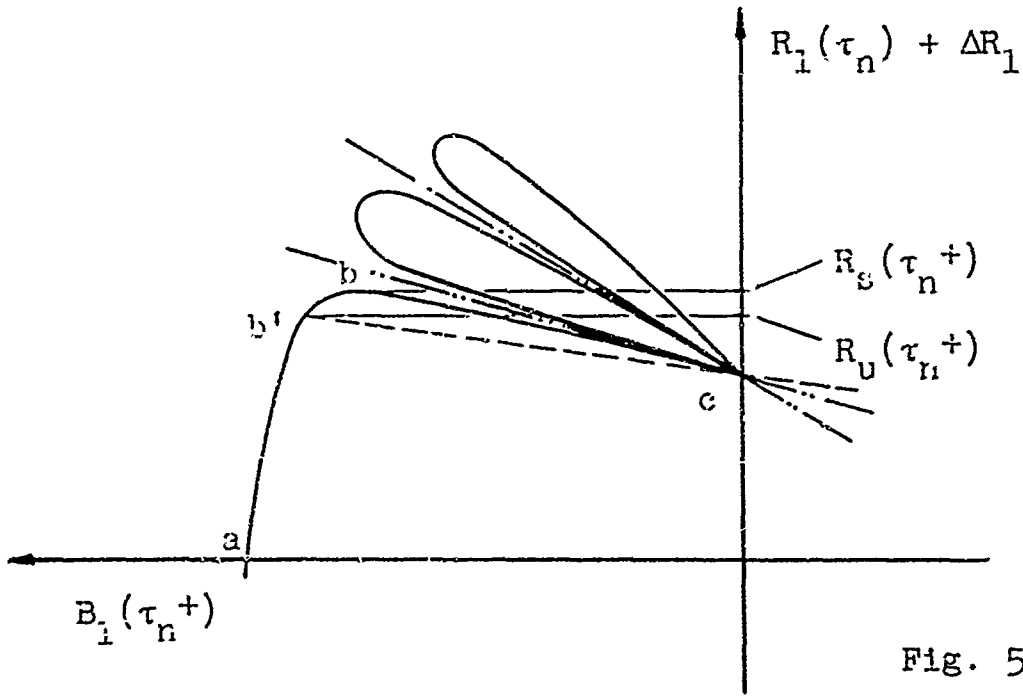


Fig. 5.7

and it can be seen by comparing this to equation (5.16) that all real solutions of equation (5.16) must fall within the dashed curve as shown.

If $R_1(\tau_n) < \left[R_1(\tau_n) \right]_{cr}$ then an unbuckled equilibrium position exists and is represented by a point on the arc ab. $B_1(\tau_n)$ can be calculated from equation (5.16) and the other modes then calculated from equation (5.5). Following the same procedure as was used when only two modes were excited $S(\tau_n^+)$, $S_1(\tau_n^+)$, $S_r(\tau_n^+)$ and $S_m(\tau_n^+) = 0$ can be calculated, and equations (5.8) then give the governing system of equations for the time $\tau = \tau_n^+$.

Again two possible solutions exist, the first with $B_m(\tau_n^+) = 0$ which gives

$$B_1(\tau_n^+) \left[1 + B_1^2(\tau_n^+) + \sum_{k=r} k^2 \left(\frac{\left(\frac{-(R_k(\tau_n) + \Delta R_k)}{k^2} + k^2 (A_k - S_k(\tau_n^+)) \right) B_1(\tau_n^+)}{- (R_1(\tau_n) + \Delta R_1) - A_1 + S_1(\tau_n^+) + (k^2 - 1) B_1(\tau_n^+)} \right)^2 - A_1^2 - \sum_{k=r} k^2 A_k^2 + S(\tau_n^+) \right] = - (R_1(\tau_n) + \Delta R_1) - A_1 + S_1(\tau_n^+) , \quad (5.17)$$

and $B_r(\tau_n^+)$ as given by equation (5.10).

The second solution with one $B_m(\tau_n^+) \neq 0$ has $B_1(\tau_n)$ and $B_r(\tau_n^+)$ as given by equations (5.13) and (5.14)

respectively, and $B_m(\tau_n^+)$ is governed by

$$m^2 B_m^2(\tau_n) = -m^2 + \sum_{k=1,r} k^2 A_k^2 - S(\tau_n)$$

$$- \sum_{k=1,r} k^2 \left(\frac{-\left(\frac{R_k(\tau_n) + \Delta R_k}{k^2} + k^2(A_k - S_k(\tau_n^+))\right)^2}{k^2 - m^2} \right) \quad (5.18)$$

where $m \neq 1, r$

If the second mode is excited, then as before $B_m(\tau_n^+)$ will always remain zero, but if the second mode is not excited, $B_m(\tau_n^+) \neq 0$ where $m = 2$ may be a possible solution.

Fig. 5.7 shows equations (5.13) and (5.17) for the case $m = 2$, i.e. the second mode is not excited. Thus if b' falls along the portion ab as shown, $R_u(\tau_n^+)$ is the critical loading, but if b' falls along bc or does not exist then $R_c(\tau_n^+)$ is critical.

It can be seen that the only difference in the solution of the case where many modes are excited, as compared to the case of two excited modes, is that the order of the polynomial that determines $B_1(\tau)$, equations (5.16) or (5.17), is raised by two for every additional excited mode. While this raises the possibility of having more equilibrium positions, it is noted that these additional positions are not unbuckled stable equilibrium positions, and so in the actual evaluation of the critical buckling load they are not a factor. The fact that the polynomial is of higher order causes some

increase in the work required to calculate the unbuckled equilibrium position, but this is the essential difference between the two cases.

Figs. 5.8 and 5.9 show the ordinate $B_1(\tau)$ plotted against τ , the dimensionless time parameter, for a fluid and a solid material respectively. Aside from the fundamental difference in the two figures, caused by the fact that for loads below a certain value the arch made of a solid material reaches a stable equilibrium value as $\tau \rightarrow \infty$, the response of the two cases is qualitatively the same. It is to be

noted that for small values of asymmetry $\frac{A_2}{A_1} < 0.001$

the ordinate is nearly identical with that of the sinusoidal case until the critical condition is approached, at which time it starts to diverge rather rapidly with subsequent failure.

Figs. 5.10 and 5.11 are plots of the critical buckling time vs. the applied load for various amount of asymmetry in the second mode. Of particular interest is the large decrease in the critical time for very small amounts of this asymmetry. As pointed out previously the effect of exciting the third or higher mode is not as great as exciting the second mode, but the character of the response is the same as that shown in Figs. 5.8 to 5.11.

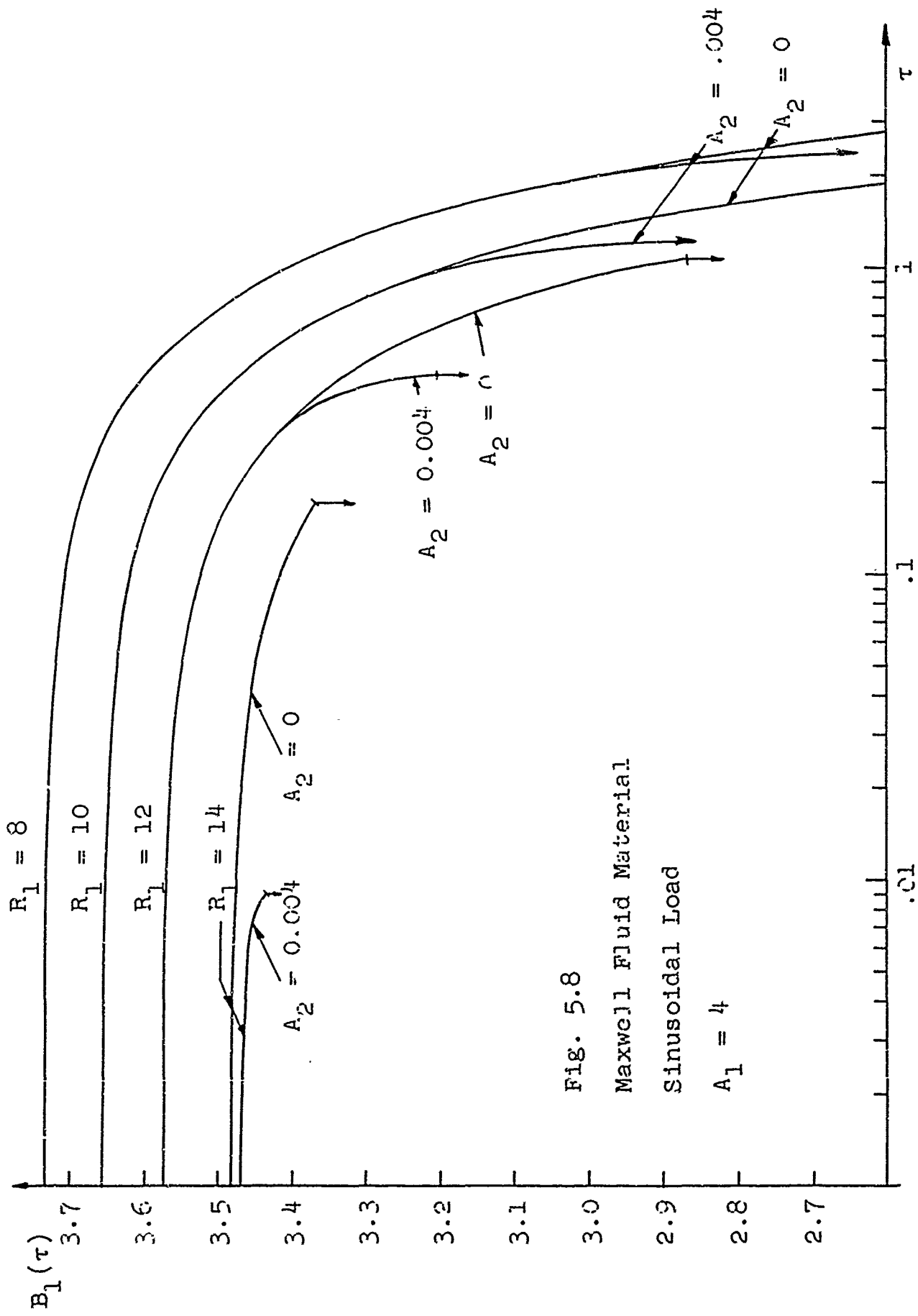


Fig. 5.8
 Maxwell Fluid Material
 Sinusoidal Load
 $A_1 = 4$

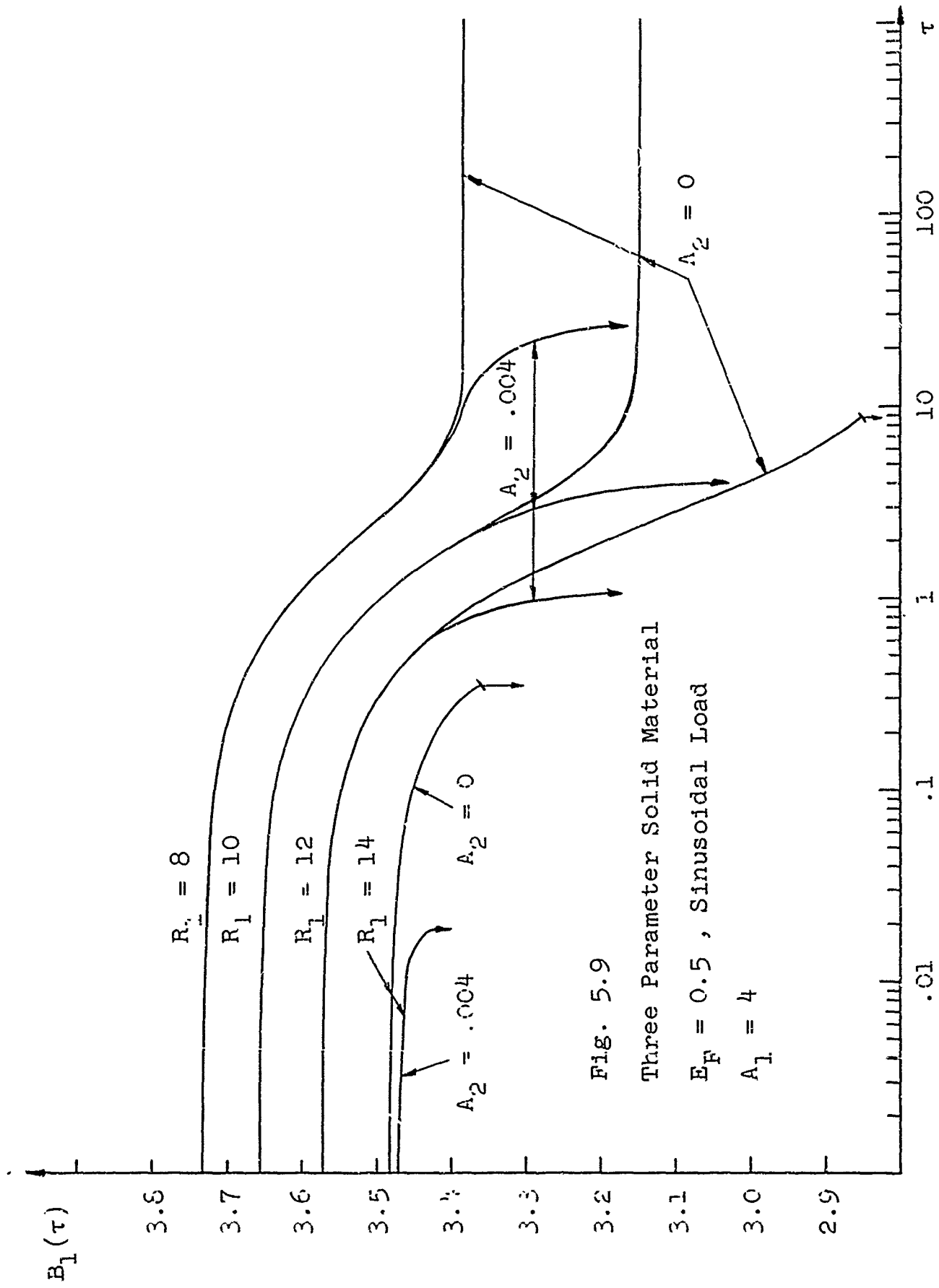


Fig. 5.9
 Three Parameter Solid Material
 $E_F = 0.5$, Sinusoidal Load
 $A_1 = 4$

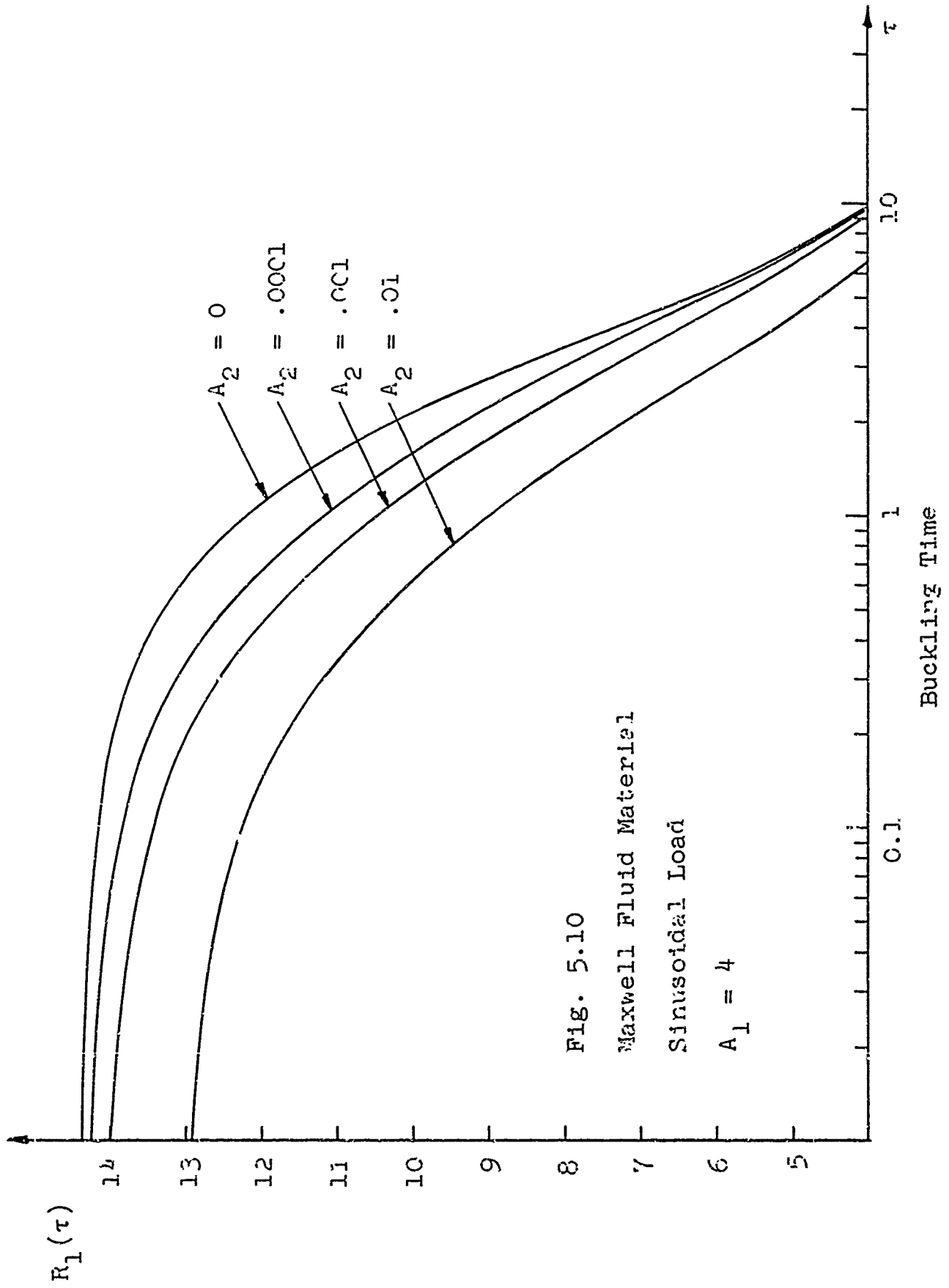


Fig. 5.10
 Maxwell Fluid Material
 Sinusoidal Load
 $A_1 = 4$

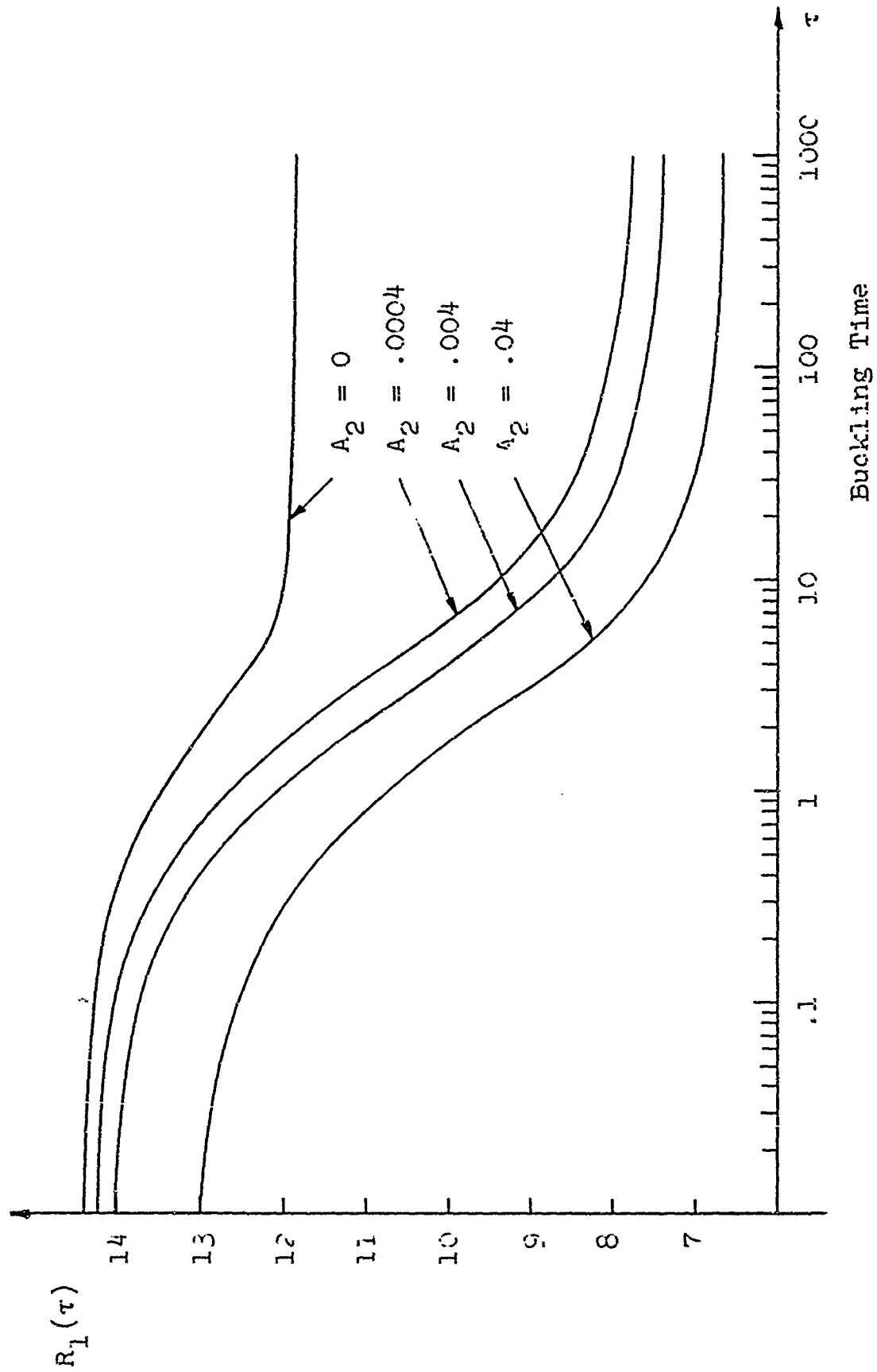


FIG. 5.11 Three Parameter Solid Material $E_F = 0.5$
 Sinusoidal Load $\Lambda_1 = 4$

Chapter VI Long-time Solution for a Viscoelastic Solid
Material

If the arch is made of a viscoelastic solid material, and the loading approaches a constant as τ becomes large, then there is a possibility of the deflection reaching some final stable value as $\tau \rightarrow \infty$.

Letting τ_F denote τ as it becomes very large, equations (3.21) can be written as

$$B_m(\tau_F)$$

$$\left\{ m^2 + \sum_{k=1}^{\infty} k^2 (B_k^2(\tau_F) - A_k^2) + \int_{0^+}^{\tau_F} \frac{E'(\tau_F - \xi)}{E_0} \sum_{k=1}^{\infty} k^2 (B_k^2(\xi) - A_k^2) d\xi \right\}$$

$$= \frac{-R_m(\tau_F)}{m^2} + m^2 \left\{ A_m - \int_{0^+}^{\tau_F} \frac{E'(\tau_F - \xi)}{E_0} (B_m(\xi) - A_m) d\xi \right\} \quad (6.1)$$

$$m = 1, 2, 3, \dots$$

In the evaluation of the integrals it is to be noted that $B_m(\xi)$ is essentially constant and equal to $B_m(\tau_F)$ for $\xi \rightarrow \tau_F$. For ξ small $B_m(\xi)$ varies but $E'(\tau_F - \xi) \rightarrow 0$ since $(\tau_F - \xi)$ becomes very large. Therefore in the range of ξ where $E'(\tau_F - \xi)$ is different from zero $B_m(\xi)$ is nearly constant and so can be taken out from under the integral sign. Thus to a good approximation

$$\int_{0^+}^{\tau_F} \frac{E'(\tau_F - \xi)}{E_0} (B_m(\xi) - A_m) d\xi = \frac{E_F - E_0}{E_0} (B_m(\tau_F) - A_m) ,$$

where $E_F = E(\infty)$. (6.2)

Similarly,

$$\int_{0^+}^{\tau_F} \frac{E'(\tau_F - \xi)}{E_0} \sum_{k=1}^{\infty} k^2 (B_k^2(\xi) - A_k^2) d\xi$$

$$= \frac{E_F - E_0}{E_0} \sum_{k=1}^{\infty} k^2 (B_k^2(\tau_F) - A_k^2) \quad (6.3)$$

Substituting equations (6.2) and (6.3) into equations (6.1) gives

$$B_m(\tau_F) \left\{ m^2 + \sum_{k=1}^{\infty} (B_k^2(\tau_F) - A_k^2) \right\} = - \frac{E_0}{E_F} \frac{R_m(\tau_F)}{m^2} + m^2 A_m \quad (6.4)$$

$$m = 1, 2, \dots$$

Equations (6.4) are identical with the equations of an elastic arch of modulus E_F under the same loading; but in the viscoelastic case they can only be used to determine the unbuckled equilibrium position denoted by the ordinates $B_m(\tau_F)$, since in their derivation it was assumed the arch was stable under the loading $R_m(\tau_F)$ and had reached a final configuration.

To check the stability at $\tau = \tau_F$, subject the arch to an additional load at $\tau = \tau_F^+$ in the same manner as was done previously in Chapters IV and V. $B_m(\tau_F)$ can be calculated from equations (6.4), considering any unexcited modes to remain zero. If an unbuckled solution of equations (6.4) does not exist, this indicates the arch has buckled at some previous finite time. On the assumption that $B_m(\tau_F)$ exists, the integrals $S(\tau_F^+)$ and $S_m(\tau_F^+)$ (see

equations (4.15) or (5.7)) can be evaluated, thus

$$\begin{aligned}
 S(\tau_F^+) &= \int_{0^+}^{\tau_F} \frac{E'(\tau_F - \xi)}{E_0} \sum_{k=1}^{\infty} k^2 (B_k^2(\xi) - A_k^2) d\xi \\
 &= \left(\frac{E_F - E_0}{E_0} \right) \sum_{k=1}^{\infty} k^2 (B_k^2(\tau_F) - A_k^2) , \quad (6.5)
 \end{aligned}$$

$$S_m(\tau_F^+) = \frac{E_F - E_0}{E_0} (B_m(\tau_F) - A_m) .$$

The governing equations for $B_m(\tau_F^+)$ then become, from equations (3.30)

$$\begin{aligned}
 B_m(\tau_F^+) &\left\{ m^2 + \sum_{k=1}^{\infty} k^2 (B_k^2(\tau_F^+) - A_k^2) + S(\tau_F^+) \right\} \\
 &= \frac{-(R_m(\tau_F) + \Delta R_m)}{m^2} + m^2 (A_m - S_m(\tau_F^+)) , \quad (6.6)
 \end{aligned}$$

$$m = 1, 2, 3, \dots .$$

The solution for this set of equations and the method of determining stability are given in Chapter IV or Chapter V, depending on the number of excited modes. If it is found that $(\Delta R_i)_{cr} < 0$, this indicates that the arch has buckled at some previous finite time.

It is to be noted that the critical load found from equations (6.6) differs from the critical load of a purely elastic arch of modulus E_0 that has the same deflected shape as the long-time solution of the viscoelastic arch under the same loading $R_m(\tau_F)$. This is due to the fact

that, although the two arches support the same load with the same deflected shape, the axial thrust and moment distribution are not the same in both cases. This arises because the moment is directly proportional to the deflection while the thrust is proportional to the square of the displacement.

In [11] it was shown that, for a uniform load on a sinusoidal arch, the effect of the higher modes, i.e. 3, 5, 7, ..., was to reduce the critical load by no more than .5% of the critical sinusoidal load. That this is not valid for the viscoelastic case can be expected from the results of Chapter V, where it is seen that near the critical buckling time the displacement of the non-sinusoidal arch differed considerably from the displacement of the sinusoidal arch (see Fig. 5.9). The reason for this can be seen from an examination of equations (5.17) and (5.18). In each of these expressions there is a series of the form

$$\sum_{k=r} k^2 \left(\frac{-\left(\frac{R_k(\tau_n) + \Delta R_k}{k^2}\right) + k^2(A_k - S_k(\tau_n^+))}{k^2 - m^2} \right)^2 \quad (6.7)$$

where r includes any excited mode other than the first.

In order to illustrate the effect of the viscoelastic material, consider the case of a uniform load on a sinusoidal arch

which has

$$R_r(\tau) = \frac{R_1(\tau)}{r} \quad , \quad r = 3, 5, 7, \dots$$

$$= 0 \quad , \quad r = 2, 4, 6, \dots \quad ,$$

and $A_r = 0 \quad , \quad r \neq 1 \quad .$

Substituting these into the series (6.7) results in

$$\sum_{k=3,5,7,\dots} \frac{k^2}{(k^2 - m^2)^2} \left(-\frac{(R_1(\tau_n) + \Delta R_1)}{k^3} - k^2 S_k(\tau_n^+) \right)^2 \quad (6.8)$$

In the elastic case $S_k(\tau) = 0$ and the series (6.8) is reduced to

$$\sum_{k=3,5,7,\dots} \frac{(R_1(\tau_n) + \Delta R_1)^2}{k^4 (k^2 - m^2)^2} \quad (6.9)$$

which is a very rapidly converging series. For $m = 2$

$$\sum_{k=3,5,7} \frac{1}{k^4 (k^2 - 4)^2} = 4.977 \times 10^{-4} ,$$

and so the effect of the higher modes on the elastic critical load is seen to be negligible. However, for the viscoelastic case $S_r(\tau_n^+) \neq 0$, and so the second term of the series (6.8) leads to an expression of the form

$$\sum_{k=3,5,7} \frac{k^6}{(k^2 - m^2)^2} S_k^2(\tau_n^+) , \quad (6.10)$$

which could be divergent, depending on the values of $S_r(\tau_n^+)$. While it is not possible to express explicitly $S_r(\tau_n^+)$ as a function of r , it is seen that in the long-time solution $S_r(\tau_n^+)$ varies directly as $B_r(\tau_F)$ (see equation (6.5)), and that

$$B_r(\tau_F) = \frac{-\frac{E_F R_1(\tau_F)}{E_O r^3}}{\frac{-R_1(\tau_F) + A_1}{B_1(\tau_F)} + (r^2 - 1)} \quad (6.11)$$

$$r = 3, 5, 7 \dots$$

Equations (6.11) are derived from equations (6.4) for a uniform load on a sinusoidal arch. Thus it is seen that for large r , $B_r(\tau_F)$ varies as $\frac{1}{r^5}$ and so the convergence of the series (6.10) is assured. The fact remains however, that the series (6.8) may not be negligible since some of the lower terms may have appreciable magnitude, and cannot be neglected in the calculations. Added to this is the fact that the terms $S(\tau_F^+)$ and $S_r(\tau_F^+)$ appear in other ways in equations (5.17) and (5.18) and must be accounted for.

Figs. 6.1 to 6.4 show the effect of E_F and $R_1(\tau_F)$ on the buckling load of an arch with initial rise $A_1 = 4$. Compared to Fig. 6.1, which is the purely sinusoidal case, the other figures show a very rapid decrease in the critical load as $R_1(\tau_F)$ increases. This can be attributed to the fact that the amplitude of the higher modes in the unbuckled configuration increases very rapidly as the load approaches the critical load (see Fig. 5.2).

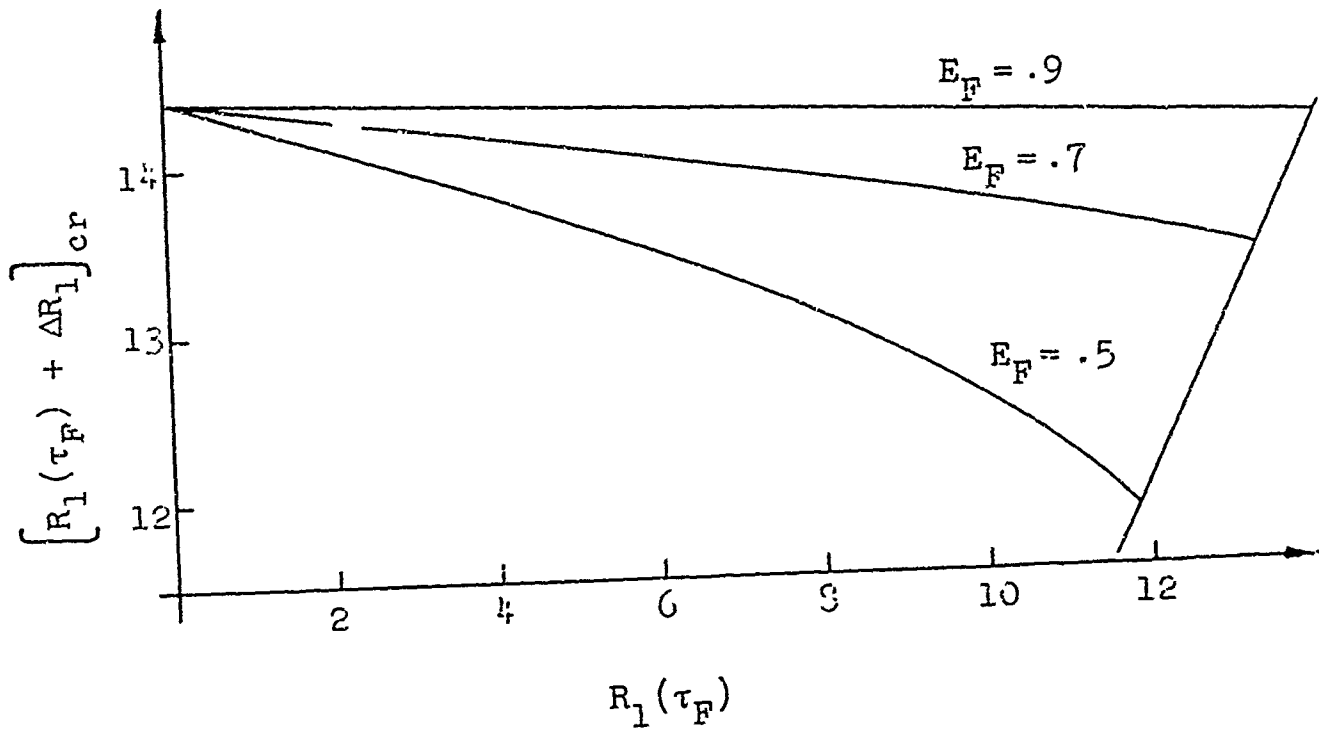


Fig. 6.1 Three Parameter Solid Material Sinusoidal Arch $A_1 = 4$, Sinusoidal Load

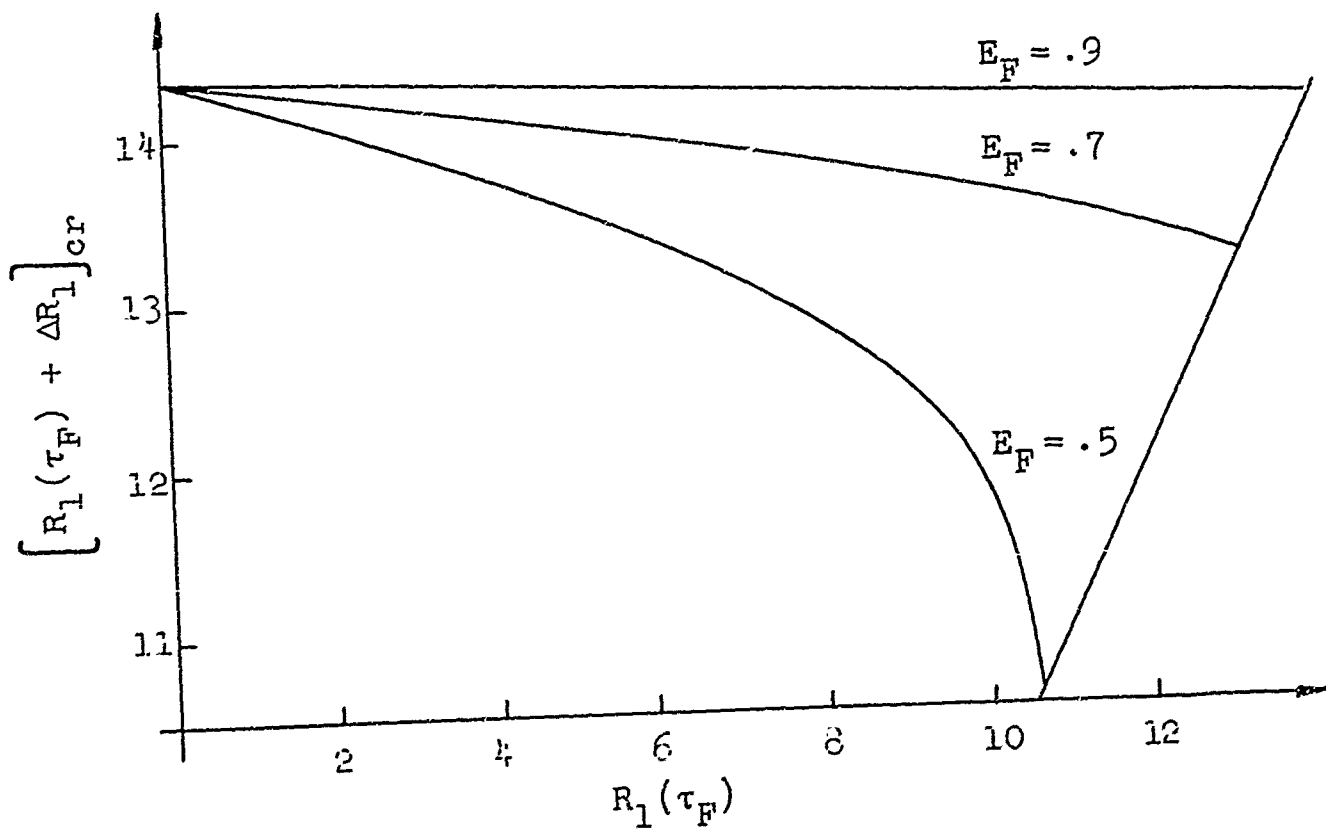


Fig. 6.2 Three Parameter Solid Material Sinusoidal Arch $A_1 = 4$, Uniform Load

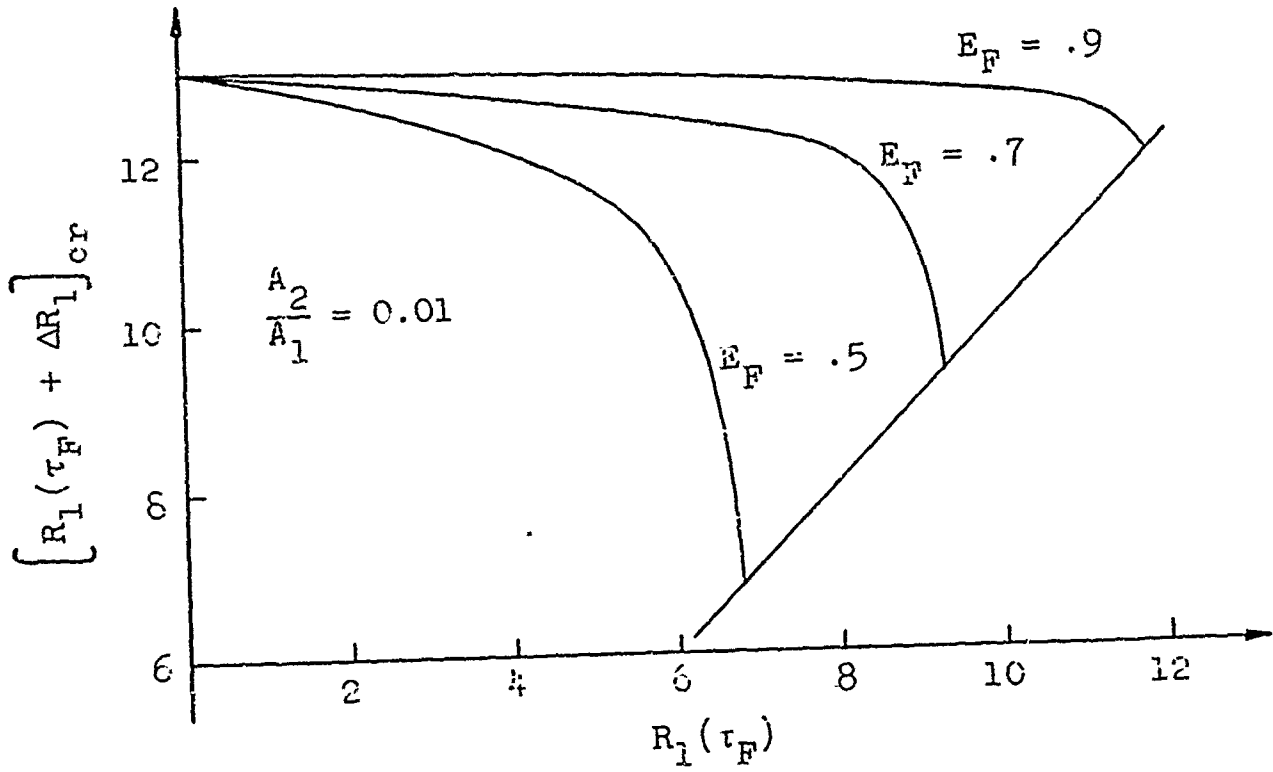


Fig. 6.3 Three Parameter Solid Material
Nonsinusoidal Arch $A_1 = 4$
Sinusoidal Load

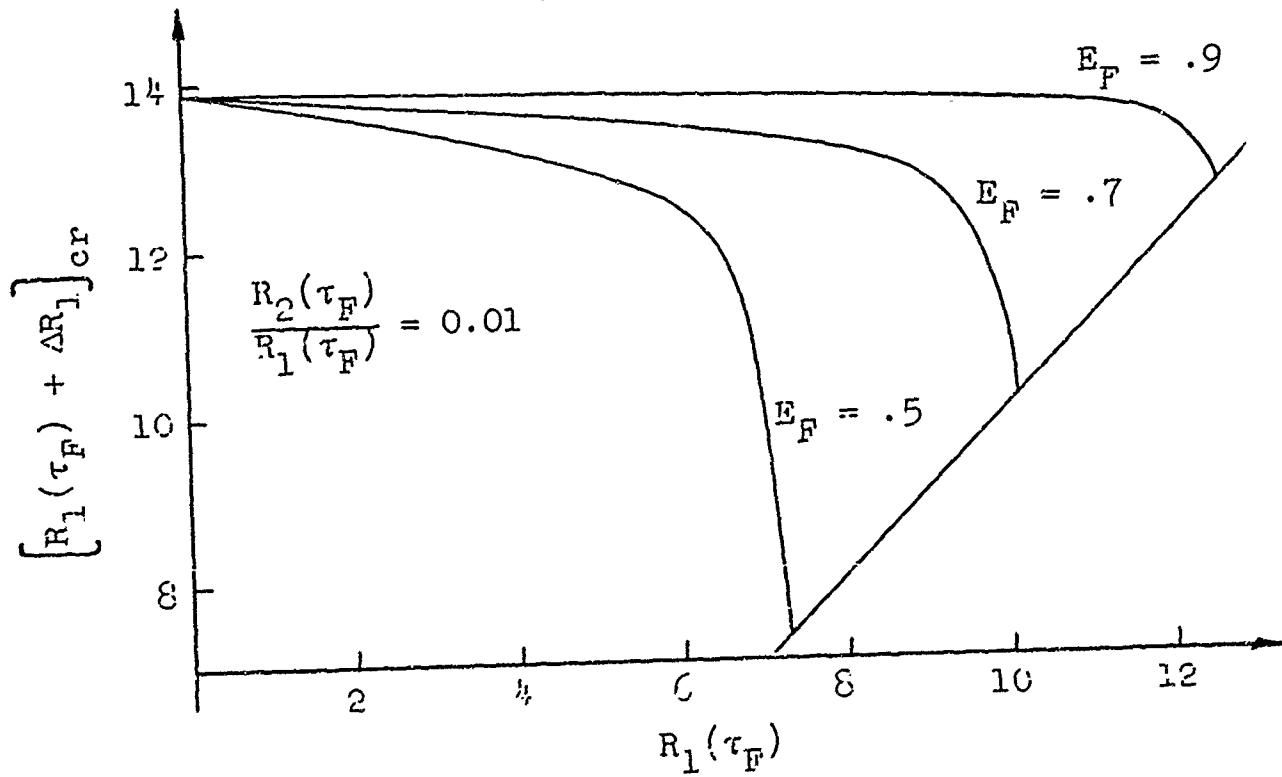


Fig. 6.4 Three Parameter Solid Material
Sinusoidal Arch $A_1 = 4$
Nonsinusoidal Load

Chapter VII General Features of the Numerical Solution

The numerical integration and solution of the roots of the algebraic equations were performed on the B-5000 digital computer at Stanford University.

In the numerical integration of integrals of the type

$$\int_{0^+}^{\tau} \frac{E'(\xi)}{E_0} f(\xi) d\xi \quad (7.1)$$

it is advantageous to use a variable time step if the form of the functions $E(\tau)$ and $f(\tau)$ are of the requisite type. $E'(\tau)$ varies quite rapidly for τ small but as τ becomes large $E'(\tau)$ approaches zero. In this problem, where $f(\tau)$ represents functions of the type $(B_m(\tau) - A_m)$, it is possible to draw several conclusions regarding the behavior of $f(\tau)$ if the loading functions $R_m(\tau)$ are sufficiently smooth. For τ small $f(\tau)$ will vary quite rapidly, regardless of the type of viscoelastic material, but for τ large the material property makes a considerable difference. For a fluid material it is expected that $f(\tau)$ would continue to vary quite rapidly until failure takes place, especially if the time at failure is quite small. On the other hand if the material is a viscoelastic solid the variation at large times will be quite small, except near the critical time.

In order to take advantage of these facts and reduce the computing time, a logarithmic time step increment was

used (see [15]) until the critical time was found, at which time the program reverted back to the last known stable time and a smaller time step introduced. In this manner small time steps were used for τ small and τ near the critical time, while larger steps were used where $E'(\tau)$ and $f(\tau)$ varied more slowly.

Among the roots $B_1(\tau)$, only the largest root of $B_1(\tau)$ is required in the analysis and so a simple iterative type solution was used. Convergence was very rapid for solutions near the point a of Fig. 4.1 but became slower as the equilibrium value approached b , at which point the program would not converge.

If the program would not converge a check was made to insure that no unbuckled equilibrium solutions existed, as this constitutes one possible mode of failure. The second possible type of failure, that of an unexcited mode becoming non-zero, is easily checked by calculating $B_1(\tau)$ on the basis of $B_m(\tau) \neq 0$ (see for example equation (4.9)), then if the $B_1(\tau)$ found in this manner is greater than the $B_1(\tau)$ found from the iterative solution, the arch is unstable.

The time step increments and the allowable tolerance in the iterative solution were adjusted so that the solution for $B_1(\tau)$ was accurate to at least four significant digits in all the test cases considered. The maximum computer time needed was less than one minute for any one problem including a case where ten modes were excited and the maximum time taken

to be 1000.

In Chapter VI there are no time integrations to be performed, but in order to find the critical load for equations (6.6) it was necessary to use a double iterative procedure. One iterative procedure is required to determine the unbuckled equilibrium position, and a second is then required to find the critical buckling load. Thus, although the programming is quite simple, considerable machine time is required in its execution.

REFERENCES

1. Timoshenko, S. P. and Gere, J. M., THEORY OF ELASTIC STABILITY, 2nd Edition, McGraw-Hill.
2. Kempner, J., "Viscoelastic Buckling", HANDBOOK OF ENGINEERING MECHANICS, ed. W. Flügge, McGraw-Hill, 1962.
3. Kempner, J. and Hoff, N. J., "Behavior of a Linear Viscoelastic Column", Appendix II to Hoff, N. J., Structural Problems of Future Aircraft, Proceedings of the Third Anglo-American Aeronautical Conference, the Royal Aeronautical Society, London, England, 1952, p. 110.
4. Kempner, J. and Pohle, F. V., "On the Nonexistence of a Finite Critical Time for Linear Viscoelastic Columns", Journal of the Aeronautical Sciences, Vol. 20, No. 8, p. 572, August 1953.
5. Hilton, H. H., "Creep Collapse of Viscoelastic Columns with Initial Curvatures", Journal of the Aeronautical Sciences, Vol. 19, No. 12, p. 844, December 1952.
6. Lin, T. H., "Stresses in Columns with Time-Dependent Elasticity", Proceedings of the 1st Midwestern Conference on Solid Mechanics, 1953.
7. Lin, T. H., "Creep Stresses and Deflections of Columns", Journal of Applied Mechanics, Vol. 23, No. 2, p. 214, June 1956.
8. Hilton, H. H., "On the Nonexistence of Finite Critical Times for Generalized Linear Viscoelastic Columns with Arbitrary Initial Curvatures", Journal of the Aerospace Sciences, Vol. 28, No. 8, August 1961.
9. Goodier, J. N. and Ramsey, H., "Problems of Related Elastic and Viscoelastic Buckling in One and Two Dimensions", Stanford University Engineering Mechanics Technical Report No. 133, July 1962.
10. Pian, T. H. H., "Creep Buckling of Curved Beams Under Lateral Loading", Proceedings, Third U. S. National Congress of Applied Mechanics (Brown University) (ASME) 1958.
11. Fung, Y. C. and Kaplan, A., "Buckling of Low Arches or Curved Beams of Small Curvature", NACA Technical Note 2840, November 1952.

12. Bland, D. R., THE THEORY OF LINEAR VISCOELASTICITY, Pergamon, 1950.
13. Lee, E. H., "Viscoelastic Stress Analysis", First Symposium on Naval Structural Mechanics, ed. J. N. Goodier and N. J. Hoff, Pergamon, 1950.
14. Lee, E. H. and Rogers, T. G., "Solution of Viscoelastic Stress Analysis Problems Using Measured Creep or Relaxation Functions", Journal of Applied Mechanics, Vol. 30, p. 127, July 1963.
15. Lee, E. H. and Rogers, T. G., "On the Finite Deflection of a Viscoelastic Cantilever", Proceedings, Fourth U. S. National Congress of Applied Mechanics (Berkeley) (ASME) 1962.
16. Hoff, N. J., "A Survey of the Theories of Creep Buckling", Stanford University Aeronautical Engineering Report No. 80, June 1958. Also Proceedings, Third U. S. National Congress of Applied Mechanics (Brown University) (ASME) pp. 29-49, 1958.
17. Gjelsvik, A. and Bodner, S. R., "An Investigation of the Energy Criterion in Snap Buckling Problems with Application to Clamped Arches", Brown University Engineering Technical Report No. 28, February 1962. Also "The Energy Criterion and Snap Buckling of Arches", Proceedings of the A. S. C. E., Vol. 88, No. EM5, October 1962.